TRANSIENT RESPONSE OF MECHANO-ACOUSTICAL NETWORKS

By

T. V. SESHADRI

Bachelor of Engineering
Madras University
Madras, India
1958

Master of Engineering
Indian Institute of Science
Bangalore, India
1961

Submitted to the Faculty of the Graduate College
of the Oklahoma State University
in partial fulfillment of the requirements
for the Degree of
DOCTOR OF PHILOSOPHY
May, 1968

TRANSIENT RESPONSE OF

MECHANO-ACOUSTICAL

NETWORKS

Thesis Approved:

Richard L. Lowery
Thesis Adviser

J. K. Dutton

Karl N. Reid

James R. Partin

N. Durham
Dean of the Graduate College

ACKNOWLEDGMENTS

I am highly indebted to my academic adviser and doctoral committee chairman, Dr. R. L. Lowery, whose intuition, encouragement, and a sound background in sonic boom studies helped make this work possible. Due regard is paid to him for his help during my entire stay in Stillwater. The financial support of the author by NASA during the period of this work is appreciated.

Thanks are due to Drs. K. N. Reid, J. R. Partin and J. R. Norton for serving on my doctoral committee and for editing this thesis. Dr. G. W. Zumwalt is especially thanked for his many helpful suggestions.

Thanks are also due to Messrs. D. J. Bayles and R. Kearl for their help in the experimental work. Mr. Eldon Hardy is thanked for his drafting and Mrs. Thomas Lee is thanked for typing the manuscript.

TABLE OF CONTENTS

LIST OF TABLES

LIST OF FIGURES

LIST OF SYMBOLS

x,y	Refer to the x,y Directions in Rectangular Co-ordinate System
$\ddot{x},\dot{x}$	Acceleration and Velocity
h	Thickness of the Panel
m	Mass
a,b	Dimensions of the Panel
E	Young's Modulus
D	Flexural Rigidity of the Panel
$w,\dot{w}$	Displacement and Velocity
ρ	Density
γ	Ratio of Specific Heats
τ	Duration of N-Wave or Shear Stress
υ	Co-efficient of Kinematic Viscosity or Poisson's Ratio
ω,f	Frequencies in rps and cps
q	Intensity of Pressure Loading
T	Period
μ	Co-efficient of Kinematic Viscosity or Mass of Material per Unit Volume
A	Area
L	Length
F	Force or Stress Function
C	Damping Factor
ζ	Damping Ratio
σ	Stress

e	Strain or Non-linearity Co-efficient
k	Stiffness
p	Pressure
u	Displacements of a Bar
V	Volume
c	Speed of Sound

CHAPTER I

INTRODUCTION

The immediate problem confronting the designers of the Supersonic Transport is the structural damage caused by the sonic booms. The booms created by these planes will usually have an overpressure of 2.5 psf and a period of 0.4 seconds, but during some maneuvers these can be as high as 4 psf and 0.5 seconds respectively. Several controlled and uncontrolled flight tests conducted in the United States and Canada prove the capability of the sonic boom in causing structural damage either due to a too large an overpressure or to the repeated exposure to booms.

In the flights over Washington, Ohio, Cedar City, Utah, and Ottawa, Canada the sonic boom caused by pilots' errors shattered several windows. The damage to the unfinished Ottawa terminal was estimated as 300,000 dollars. In the tests conducted in Oklahoma City one of the showcase windows of the Kinney Shoe Store broke. There were reports of nail popping, paint and plaster cracking due to the repeated application of loads by the sonic boom. In the recent experiments by NASA at the Edwards Air Force Base a controlled flight shattered a glass window in the U. S. Post Office and created cracks and broke another window in the same building. From the data obtained from these tests it is clear that the overpressure as a static load was not responsible for the failure of glass as it was only 10% of the wind load for which it is

designed. The building enclosures behave as Helmholtz resonators and drive the flexible members such as the window to high amplitudes, especially when the natural period of the window is equal to the natural period of excitation. It is therefore necessary to study the response characteristics of acoustical networks for transient loads to find the maximax response. In addition to sonic boom loads, this study will be useful in the response analysis of building structures subject to other transient loads such as explosions, rocket launchings, gusts, and blast loads.

A building structure, because it is composed of several rooms, inter-connecting hallways, doors and windows, is complicated to analyze mathematically. It has to be reduced to an equivalent system which adequately represents the behavior of the original system. The response of a dynamical system depends on the damping ratio of the system. Every physical system possesses some energy dissipating mechanisms. From the data obtained from the Oklahoma City tests it is known that the pressure oscillations are not sustained for a long time. Even though the damping ratio does not affect the response due to transient loads as much as it does the response to steady state, its effect is pronounced in the former also. A damping ratio of 5% could reduce the maximax response by as much as 25%. Therefore in order to find the transient response of acoustical networks the types of damping present in them should be identified. The response is easily obtained once the equivalent viscous damping ratio is known.

The maximax response of any system depends on its components. By suitably modifying them any desired response can be obtained. The components of an acoustical system are to be changed within practical

limits and the critical system has to be found. The maximax of this system is the maximum that can be expected for a given sonic boom type input. Thus an upper bound for the response can be obtained. This is very useful in the design of the components of the acoustical networks, especially the glass windows.

If the deflection of the panel to the transient excitation is much greater than the thickness, some refined theories have to be used to find the dynamic response.

In general the main objectives of this work can be summarized as:

1. To represent the building structures which are mechano-acoustical systems by equivalent mechanical systems which preserve the characteristics of the original system adequately.
2. To identify the types of damping present in representative buildings and thus to estimate a lower bound for the net equivalent viscous damping ratio.
3. To find the maximax response of multi-degree of freedom systems as a function of its parameters.
4. To find the most critical multi-degree of freedom system and thus to find a worst practical acoustical system.
5. To get an upper bound for the stresses in the glass windows for a given sonic boom type input using both linear and non-linear theory, and
6. To compare the maximax response calculated with the experimental data obtained from tests conducted at the Edwards Air Force Base.

CHAPTER II

LITERATURE REVIEW

Several authors have discussed in general the damping ratio of Helmholtz resonators, the transient response of linear systems, resonators and some specific non-linear systems. But no literature is available on the general design of acoustical systems subject to sonic booms.

Rayleigh (29) has described the various loss mechanisms associated with a resonator such as radiation, viscous and heat conduction. He concluded for low frequency the heat conduction losses are negligible. Samulon (31) has analytically found the losses due to the viscosity of the air in the neck of the resonator. He found that the viscous losses were the main loss mechanisms for very narrow necks. He assumed the flow of air in the neck was similar to the flow in a pipe. Ingard (13) investigated the near field of a resonator exposed to a plane wave using the acoustic equation and concluded that the damping due to heat conduction was negligible. Mangiarotty (20) has derived expressions for the acoustic radiation damping of a panel vibrating in its fundamental mode. He assumed the panel to be a piston vibrating in an infinite baffle. For a uniform damping pressure he found the damping was dependent only on the density of the surrounding medium and the aspect ratio of the panel for a given material. The assumption of non-uniform damping pressure does not change the results very much

especially for panels very small compared to the wave-length. Fitzgerald (11) has discussed the internal damping of ceramics and glass using the hysteresis curves. He concluded that the internal damping of them was comparable to that of the metals. Marin and Rindone (21) have given experimental results for the hysteresis damping of glass rods. The damping was given in terms of the quality factor Q.

Several authors (36, 12) have studied the transient response of simple oscillators. There is little literature on the transient response of multi-degree of freedom systems. The work so far done has been confined, due to mathematical difficulty, to particular cases only. Hence, there is great need to solve this problem in general. Many investigators studied the transient response of continuous systems such as beams and plates. Cheng (5) has discussed the dynamic amplification factor developed due to an N-wave excitation on beams and plates. He used the Fourier series to solve the partial differential equations and concluded that for the deflection, the contribution by higher modes could be neglected. Crocker (8) has found analytically and experimentally the transient response of panels to several forms of excitation pulses. He has arrived at the same conclusion that the fundamental mode contribution adequately represented the total response for displacement.

The work on the general transient response of a non-linear system is also limited. Fung and Barton (12) have discussed the effect of non-linearity in a single degree of freedom system. They solved the problem in terms of the loading ratio, that is the ratio of the loads in the linear and the non-linear system to produce the same deflection. Ergin (10) found the response of a simple non-linear oscillator by a

bi-linear approximation method. The load-deflection curve was assumed to be made up of two straight lines such that the mean error squared was a minimum. Thomson (36) has found the shock spectra of an elasto-plastic non-linear system and has concluded that the response of this system was less than the corresponding linear system.

In order to determine whether a sonic boom will cause failure of glass windows the failure mechanisms of glass should be known. Kornhauser (16) has discussed the impact sensitivity method to predict the structural failure due to elastic and plastic deformation. Parrot (26) in his experimental study on the failure of glass due to sonic booms has shown that the failure depended on many variables such as the shape, size, edge restraints, age and imperfections. It is difficult to evaluate the effects of all these variables separately. The fatigue of glass was experimentally studied by Baker and Preston (1). They concluded that there was considerable difference between metal fatigue and glass fatigue. In fact, according to them the endurance limit of glass was only a little less than the normal breaking stress.

When the panel size and the load increase, the deflection is much greater than the thickness and the linear theory is no longer valid. So a static and dynamic analysis of plates with large deflections have to be made. Kaiser (15) has discussed the reduction of the non-linear differential equations to a system of linear equations. He solved only for a particular case of a parameter and did not discuss in great detail the convergence of the solution. Wang (39) continued the work of Kaiser and solved the system of linear equations using the relaxation and successive approximation methods. Herrmann and Chu (6) have studied the steady state vibration of large plates. They found that

the period decreased very rapidly with the amplitude of oscillation. Eisley (9) has discussed the free and steady state forced vibrations of thin plates. He used the Galerkin procedure to solve the Von-Karman equations assuming a single mode representation. The response was similar to that of a simple oscillator with hard springs.

The literature on the transient response of buildings subject to sonic boom input for general cases is scarce. The work done so far is mostly experimental. The theoretical work done on Helmholtz resonators explains the resonance effects in building enclosures but does not deal with the stresses in the flexible structures such as windows. Simpson (32) analyzed a simple Helmholtz resonator for transient loads and concluded that for dimensions smaller than the wave-length, the resonator could be assumed as a lumped system. Reddy (30) analyzed the transient response of a coupled resonator. He was mainly interested in the pressure magnification. For a favorable combination he obtained a magnification as high as 20. Whitehouse (40) found the response of a panel coupled to a resonator experimentally. He concluded that the total response could be represented by the fundamental mode contribution. In all the above work only some particular acoustical systems were analyzed. They do not necessarily represent the critical cases. Further, the damping ratios used were arbitrary. Even though the deflection was much greater than the thickness, linear theory was used. It is therefore necessary to find the maximum upper bound for the stresses that can be attained by a window subject to a given sonic boom taking into account the damping, number of degrees of freedom, the non-linear and membrane effects.

CHAPTER III

MODELING

The initial task in the analysis of a structure for static or dynamic loads is to reduce it to a form in which the desired results can be obtained with a reasonable amount of analytical work. This is necessary because the physical systems are too complicated (such as the acoustical system with many rooms, interconnecting hallways and windows) to analyze mathematically. The complexity increases if the dynamic response is required because it is a function of both time and space. Usually the mass, flexibility and energy dissipation of a physical system are distributed. Certain simplifications have to be made before a mathematical analysis is possible. The simplifications should not be such as to completely alter the characteristics of the system. The model should adequately represent the dynamic response of the structure for the particular load and at the same time the mathematical analysis should not be strenuous. This is the basic principle involved in modeling.

A vibrating panel has infinite degrees of freedom and its equation of motion is represented by a partial differential equation. The resulting response of the panel for any load is the sum of the contribution of all the modes. In order to represent the panel as a discrete system the contribution of each mode to the particular problem should be known. Whitehouse (40) has shown that, for a simply supported panel

subjected to an N- wave excitation, the fundamental mode contributes to 99.7% of the displacement and 97% of the stress. This justifies, for engineering accuracy, that a panel can be adequately represented by its fundamental mode response. The equivalent mass, stiffness and damping ratio are found by equating the kinetic, potential and damping energies. The equivalent area of the model can be found assuming the same static deflection.

Elements of the Model of a Panel

Equivalent Mass

For a simply supported panel which is uniformly loaded and vibrating harmonically the deflection in the fundamental mode is given by (37),

$$w(x,y) = w_o \, \mathrm{Sin}\pi x/a \, \mathrm{Sin}\pi y/b \cdot f(t) \tag{3-1}$$

where w_o is the deflection at the center.

The kinetic energy of the panel is

$$\tfrac{1}{2}m\dot{w}^2 = \tfrac{1}{2}\rho {w_o}^2 h \int_o^b \int_o^a \mathrm{Sin}^2 \frac{\pi x}{a} \, \mathrm{Sin}^2 \frac{\pi y}{b} \, dx \, dy \tag{3-2}$$

$$= \tfrac{1}{2} m \frac{\dot{w}_o^2}{4} \tag{3-3}$$

where $\dot{w}(x,y)$ = the velocity at any point on the surface of the panel, and

ρ = mass density of the panel

In order to have the same kinetic energy the model should have a mass m_{eq} which is one-fourth the mass of the panel.

Equivalent Stiffness

The equivalent stiffness is obtained from the potential energy. For a panel vibrating in its fundamental mode,

$$P.E. = \int_0^{w_o} \int_0^b \int_0^a q \, \text{Sin} \frac{\pi x}{a} \, \text{Sin} \frac{\pi y}{b} \, dx \, dy \, dw \tag{3-4}$$

where q is the gradually applied pressure load. The load-deflection relation is linear for small deflections and w the deflection to a pressure q can be represented by

$$q = kw \tag{3-5}$$

where k is the stiffness of the panel expressed as

$$k = \frac{\pi^6 \, D \, (a^2 + b^2)^2}{16 \, a^4 \, b^4} \tag{3-6}$$

On substitution of this in the integral and integration between the prescribed limits yields,

$$PE = \tfrac{1}{2} \frac{\pi^4 \, D \, (a^2 + b^2)^2}{4 \, a^3 \, b^3} \cdot w_o^2 \tag{3-7}$$

The equivalent spring constant k_{eq} is obtained by equating the potential energies. This gives

$$k_{eq} = \frac{\pi^4 \, D \, (a^2 + b^2)^2}{4 \, a^3 \, b^3} \tag{3-8}$$

With this k_{eq} and m_{eq} the natural frequency of the model is the same as the fundamental frequency of the panel.

Equivalent Damping Ratio

The incremental damping energy is given by

$$dE = C \, \dot{w} \, dw \tag{3-9}$$

where C = damping factor

$\dot{w}$ = velocity and

w = displacement

For a simply-supported panel vibrating in its fundamental mode

$$E = C \dot{w}_o^2 T/4 \tag{3-10}$$

where T = period.

The damping energies of the model and the panel are equated which yields

$$C_{eq} = C/4 \tag{3-11}$$

Equivalent Area

It is assumed that the force in the single degree of freedom model is in the form of a uniform pressure acting on a certain area. This assumption is valid as far as sonic boom pressure loadings on the windows is concerned. The area can be found by preserving the static deflection.

$$\frac{16\ pa^4\ b^4}{\pi^6\ D\ (a^2 + b^2)^2} = \frac{p \cdot A_{eq}\ 4\ a^3\ b^3}{\pi^4\ D\ (a^2 + b^2)^2} \tag{3-12}$$

$$A_{eq} = \frac{4}{\pi 2} \cdot A \tag{3-13}$$

The panel has thus been replaced by a single degree of freedom system which has the same static deflection, natural frequency, kinetic, potential and damping energies as the fundamental mode of the panel. It is to be seen whether this model adequately represents the fundamental mode dynamic response of the panel for all loading conditions

especially the transient.

The equation of motion for the single degree of freedom model is

$$m_{eq}\,\ddot{x} + k_{eq}\,x = p(t)\,A_{eq} \tag{3-14}$$

Since the natural frequency is preserved, the equation (3-14) can be written as,

$$\ddot{x} + \omega^2 x = \frac{16}{\pi^2 m} \cdot p(t) \cdot A \tag{3-15}$$

where A and m correspond to the panel.

Comparison of Response of Panel and the Model

The impulse response h(t) of a simply supported panel is given by

$$h(t) = \frac{1}{M_{rs}\,\omega_{rs}} \operatorname{Sin} \omega_{rs} t \tag{3-16}$$

where M_{rs} = the generalized mass in the rs^{th} mode and

ω_{rs} = the rs^{th} natural frequency.

For any other input the response can be found from the convolution integral

$$x(t) = h(t) * f(t) = \int_o^t h(t - \psi)\, f(\psi)\, d\psi \tag{3-17}$$

or in terms of generalized displacements

$$q_{rs}(t) = \int_o^t \int_o^b \int_o^a f(\psi)\, h_{rs}(t-\psi)\, \Phi_{rs}(x,y)\, dx\, dy\, d\psi \tag{3-18}$$

where Φ is the modal function. For a simply supported plate, the mode function is sinusoidal and q_{11} represents the center deflection.

Step Input

a. Panel.

If the load consists of a suddenly applied pressure

$$\left.\begin{aligned} f(t) &= p_o \quad t \geq 0 \\ &= 0 \quad t < 0 \end{aligned}\right\} \tag{3 19}$$

The response in the fundamental mode is given by

$$q_{11}(t) = \int_o^t \int_o^b \int_o^a p_o \frac{ab}{M_{11}\omega_{11}} \operatorname{Sin} \omega_{11}(t-\psi) \operatorname{Sin}\frac{\pi x}{a} \operatorname{Sin}\frac{\pi y}{b}\, dx dy d\psi \tag{3-20}$$

$$= \frac{16F}{\pi^2 m\omega^2}\left[1 - \operatorname{Cos} \omega t\right] \tag{3-21}$$

b. Model.

The equation of motion of the model for a step input is

$$\ddot{x} + \omega^2 x = \frac{16F}{m\pi^2} \tag{3-22}$$

The solution of this, obtained using Laplace Transform is

$$x(t) = \frac{16F}{\pi^2 m\omega^2}\left[1 - \operatorname{Cos} \omega t\right] \tag{3-23}$$

which is exactly the same as that obtained for the plate.

Impulse

The force is represented by

$$F(t) = \delta(t) \cdot F \tag{3-24}$$

The response of the plate from (3-18) is

$$q_{11}(t) = \frac{16F}{m\pi^2\omega} \operatorname{Sin} \omega t \tag{3-25}$$

The solution of the equation of motion of the model for an impulse

input yields an identical result.

It can be shown similarly that for a steady state sinusoidal load of F Sin αt the solution for both the panel and the model is

$$x(t) = \frac{16F}{m\pi^2}\left[\frac{1}{(\omega^2 - \alpha^2)}\right]\left[\text{Sin } \alpha t - \frac{\alpha}{\omega} \text{Sin } \omega t\right] \qquad (3\text{-}26)$$

The response for a cycle of sine pulse can be found by superposing on the above result the response due to a negative force for $t > T$.

Hence the model exactly represents the fundamental mode response of the panel for steady state or transient loads. The elements of the model are summarized in Table I.

TABLE I

ELEMENTS OF THE PANEL AND ITS MODEL

Element	Panel	Model
Mass	m	m/4
Stiffness	$\frac{\pi^6 D\,(a^2 + b^2)^2}{16\,a^3\,b^3}$	$\frac{\pi^4 D\,(a^2 + b^2)^2}{4\,a^3\,b^3}$
Damping factor	C	C/4
Damping ratio	ζ	ζ
Area	ab	$(4/\pi^2)$ab
Natural frequency	$\sqrt{\frac{\pi^4 D\,(a^2 + b^2)^2}{m\,a^3\,b^3}}$	$\sqrt{\frac{\pi^4 D\,(a^2 + b^2)^2}{m\,a^3\,b^3}}$

The Helmholtz Resonator

Since it has been proved from several sonic boom tests that ordinary building structures behave as Helmholtz resonators, it is therefore possible to predict the response of mechano-acoustical networks to sonic boom type inputs. In general the sound field of a resonator can be represented only by the acoustic equation. This is a partial differential equation similar to the equation of motion of a continuous system. When the dimensions of the structure are small compared to the wave length the behavior of pressure pulse can be described by a lumped parameter approach. For small neck areas the compressibility of air can be neglected. Since in the case of sonic boom excitation the wave length is of the order of 300 to 400 feet, most of the rooms have dimensions much less than the wave length. The lumped parameter approach is valid in those cases. Essentially, the air in the neck behaves as a mass and air in the cavity as a spring.

Mass

The mass in the simple model will have the same mass as that of the air moving back and forth near the neck. To account for an additional inertance in the neck, a correction factor has to be added to the length.

$$L_e = L + 1.45 \sqrt{A/\pi} \tag{3-27}$$

where A is the area of the neck.

Stiffness

The stiffness of the model is the same as the stiffness of the

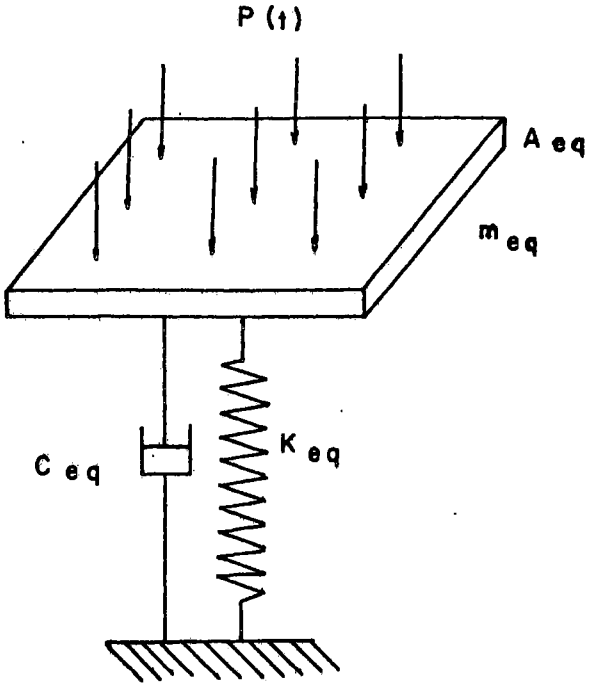

Figure 1, Lumped Model of the Panel

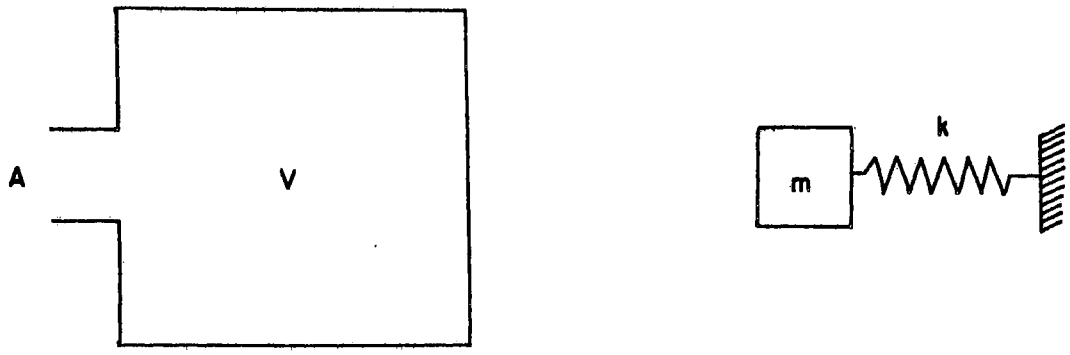

Figure 2. Helmholtz Resonator and Its Model

cavity. Since the changes take place suddenly, adiabatic expansion and compression are assumed. From the adiabatic pressure-volume relation

$$\left| dp \right| = \frac{\gamma p}{V} dV \tag{3-28}$$

The spring constant which is defined as force per unit displacement is therefore given by,

$$k = \rho c^2 A^2 / V \tag{3-29}$$

where c = speed of sound.

The equation of motion of such a model will be

$$\rho A L_e \ddot{x} + \frac{\rho c^2 A^2}{V} x = p(t) \cdot A \tag{3-30}$$

where $c\sqrt{\frac{A}{VL_e}}$ represents the natural frequency of the system.

The pressure change inside the cavity is also maintained because the change in pressure is a linear function of the change in volume or, if the area is constant, change in displacement.

Usually it is necessary to study the case of a panel coupled to a Helmholtz resonator because this represents a room with a window. The mathematical model will be a two degree of freedom system as shown in Figure 3. The elements of the model can be easily calculated from the foregoing analysis.

From the adiabatic relation the pressure change in the cavity is proportional to the change in volume.

Change in volume for the system is given by,

$$dV = A_1 x_1 - \int_0^b \int_0^a w_o \sin \frac{\pi x}{a} \sin \frac{\pi y}{b} dx\, dy \tag{3-31}$$

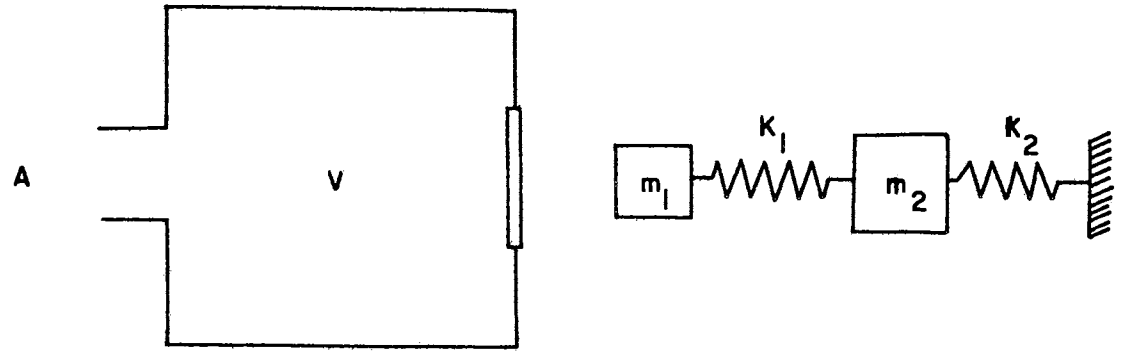

Figure 3. A Resonator with a Panel and Its Model

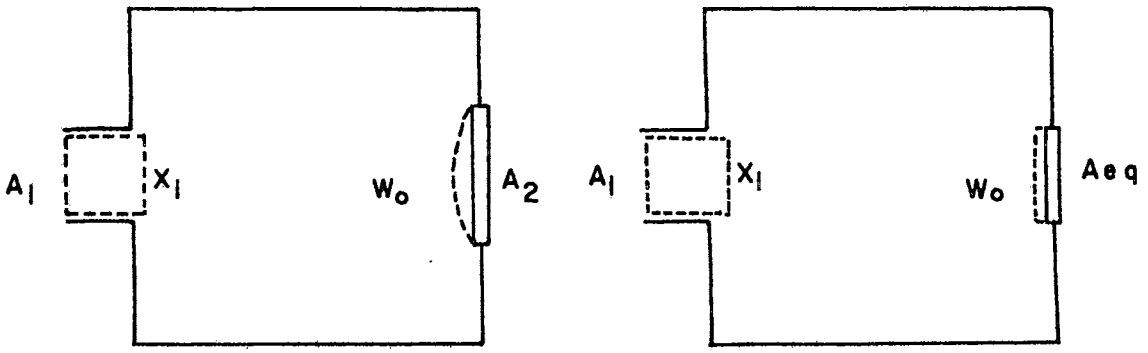

Figure 4. Displacement in the Coupled System and Its Model

$$= A_1 x_1 - w_o \cdot 4\ ab/\pi^2 \tag{3-32}$$

For the model,

$$dV = A_1 x_1 - w_o \cdot 4\ ab/\pi^2 \tag{3-33}$$

The pressure in the cavity is the same both in the system and the model because the volume changes are the same.

CHAPTER IV

DAMPING MECHANISMS IN MECHANO-ACOUSTICAL NETWORKS

Every physical system possesses some forms of damping. The maximax response of such a system depends on the damping ratio. In the preceding chapter continuous systems were replaced by discrete systems but without the knowledge of the actual damping ratios the modeling is incomplete.

Losses in a Helmholtz Resonator

The loss mechanisms in a Helmholtz resonator can be classified as

a. viscous losses
b. radiation losses
c. heat conduction losses and
d. other losses such as mechanical wall vibrations and gaseous absorption due to thermal relaxation.

Viscous Losses

The viscous loss is due to the friction to the air flow in the neck. The flow of air in the neck can be assumed to be similar to the flow of fluids in a pipe. If the neck is not circular there will be additional losses due to the sharp corners. In order to calculate the viscous losses the velocity of air in the neck should be known.

To find the damping ratio due to the boundary layer losses the

flow over a plane surface is studied. Let the fluid above the plane ($y = 0$) be made to oscillate by a force $F \cos\omega t$ per unit vertical area. Because of the friction between the fluid and the surface the velocity at the surface is zero and there is a thin boundary layer. (Figure 5)

The equation of motion is obtained considering the fluid between the two layers y and $y + dy$.

$$\upsilon \frac{\partial^2 u}{\partial y^2} + f \cos \omega t = \frac{\partial u}{\partial t} \tag{4-1}$$

where f is the force per unit mass. This equation can be solved by assuming the velocity to be a harmonic function of time. The general solution is

$$u(y,t) = u_o \left[\sin \omega t - e^{-\sqrt{\frac{\omega}{2\upsilon}} \cdot y} \sin \left(\omega t - \sqrt{\frac{\omega}{2\upsilon}} \cdot y \right) \right] \tag{4-2}$$

where u_o is equal to f/ω.

For values of $\frac{\omega}{2\upsilon} y \gg 1$, $u(y,t)$ is very nearly equal to $u_o \sin\omega t$. Therefore when $\frac{\omega}{2\upsilon} \frac{D}{2} \gg 1$ where D is the diameter of the tube considered, it can be assumed that the plate is bent in the form of a tube with little error.

The expression for the velocity can be obtained by replacing y by (R-y) in (4-2). Since $u(y,t)$ is very nearly equal to $u_o \sin\omega t$ everywhere, the root mean squared velocity u_m is $\frac{u_o}{\sqrt{2}}$.

Consider the shear force between two concentric cylinders (Figure 6),

$$F = 2 \pi y L \tau \tag{4-3}$$

where τ is the shear stress.

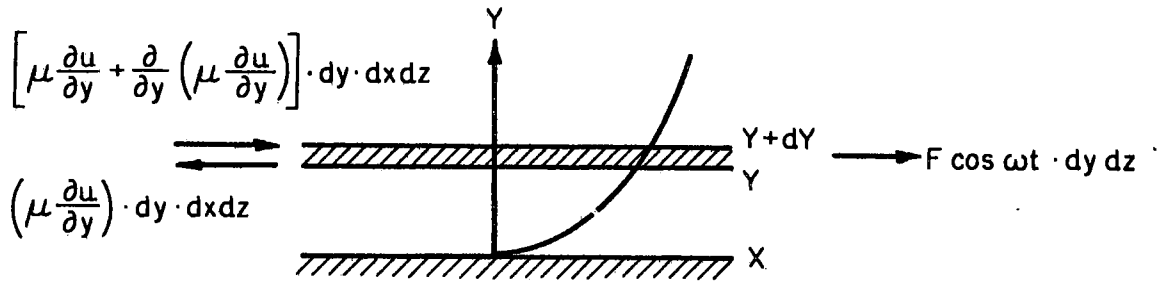

Figure 5. Boundary Layer in a Flat Plate

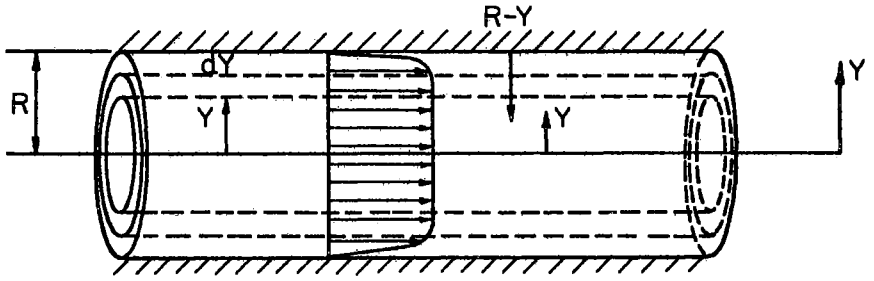

Figure 6. Velocity Distribution in a Pipe Flow

The power with which the two adjacent layers move relative to each other is given by

$$P = \int 2 \pi \mu L y \frac{du}{dy} du \tag{4-4}$$

The average power over a period of vibration is

$$\overline{P} = \frac{1}{T} \int_0^t dt \int_0^R 2 \pi y \mu L \left(\frac{du}{dy} \right)^2 dy \tag{4-5}$$

It can be shown (31) that for the fluid making sinusoidal oscillations the damping factor C is given by,

$$C = \overline{P} / u_m^2 \tag{4-6}$$

The use of this relation after integrating (4-5) yields

$$C = \frac{(2\beta R - 1 + e^{-2\beta R})}{2} \cdot 2 \pi \mu L \tag{4-7}$$

where $\beta = \sqrt{\frac{\omega}{2\upsilon}}$.

When $\beta R \gg 1$ which is true for practical cases this reduces to

$$C = 2 \pi \mu L \beta R \tag{4-8}$$

The corresponding damping ratio ζ is given by

$$\zeta = \tfrac{1}{2} \sqrt{\frac{\upsilon}{Af}} \tag{4-9}$$

where f = natural frequency of the resonator

A = area of the neck.

Radiation Losses

Another source of loss near the neck is due to the energy lost by radiation to the atmosphere. This dissipative energy can be found by assuming the mass of air in the neck of the resonator to be a piston

vibrating in an infinite baffle. The acoustic impedance of such a piston is (2),

$$\frac{p}{U} = \frac{\rho_o c}{\pi a^2}\left[1 - \frac{J_1(2ka)}{ka}\right] + \frac{j\pi\rho_o c}{2k^2\pi^2a^4} K_1(2ka) \qquad (4\text{-}10)$$

where U = volume velocity

a = radius of the piston and

k = the wave number ω/c

The resistive component of the impedance which is responsible for the energy loss is given by

$$\frac{p}{U} = \frac{\rho_o c}{\pi a^2}\left[1 - \frac{J_1(2ka)}{ka}\right] \qquad (4\text{-}11)$$

$$\text{where } J_1(2ka) = \frac{2ka}{2} - \frac{8\,k^3a^3}{16} + \frac{32\,k^5a^5}{384} + \cdots \qquad (4\text{-}12)$$

Since k, the wave number, is less than 1 for low frequencies (as is the case for excitation by sonic boom) k^5a^5 and higher powers can be neglected. Then,

$$\frac{p}{U} = \frac{\rho_o c k^2}{2\pi} \qquad (4\text{-}13)$$

Since the damping force is proportional to the velocity the resulting damping is of the viscous type. The damping force is given by

$$F = \frac{\rho_o c k^2}{2\pi} A \cdot U = C_d u \qquad (4\text{-}14)$$

where C_d is the damping factor.

This results in,

$$\zeta_{rad} = \frac{f\,A}{2cL} \qquad (4\text{-}15)$$

where ζ_{rad} is the radiation damping ratio.

Heat Conduction Losses

According to Rayleigh (29), the heat conduction losses can be included in the expression for viscous losses by using a modified coefficient of viscosity. For air, this results in a damping ratio for heat conduction losses as

$$\zeta_{hc} = 0{\cdot}265\sqrt{\frac{\upsilon}{Af}} \tag{4-16}$$

The theoretical damping ratio of a Helmholtz resonator is therefore given by

$$\zeta_{net} = \frac{fA}{2cL} + 0{\cdot}5\sqrt{\frac{\upsilon}{Af}} + 0{\cdot}265\sqrt{\frac{\upsilon}{Af}} \tag{4-17}$$

Figure 7 shows the damping ratio of resonators as a function of frequency for different necks.

Experimental Work on Helmholtz Resonators

From (4-17) and Figure 7 it is clear that for small necks the viscous and heat conduction losses are important and for wide necks the radiation losses predominate. For a medium size neck both losses contribute almost equally. In order to have all these three types of necks, neck diameters of 1.22", 2.9" and 6.5" were chosen. The resonator had an internal diameter of 13½" and had a cylindrical shape. Its height, hence the volume, could be changed by moving the wooden plugs which formed the bottom of the resonator. The bottom was sealed well by placing an aluminum plate with O-ring between the wooden plugs. The resonator was excited by a few pulses of sine wave using a tone burst generator. This was used because the natural frequency and damping ratio were calculated using visual observation and thus the repetition

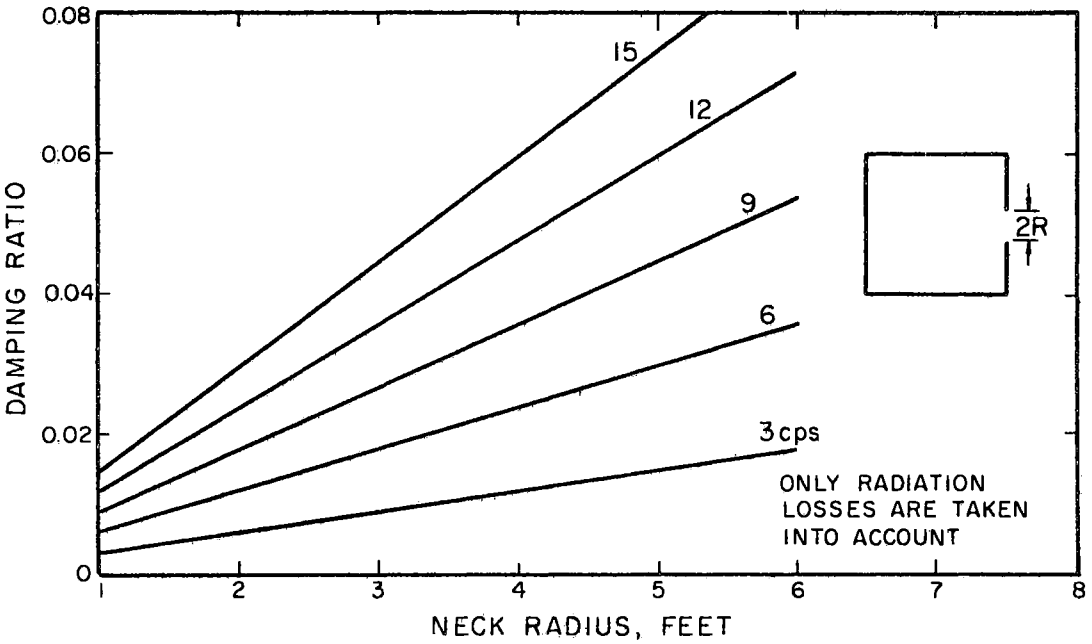

Radiation Losses

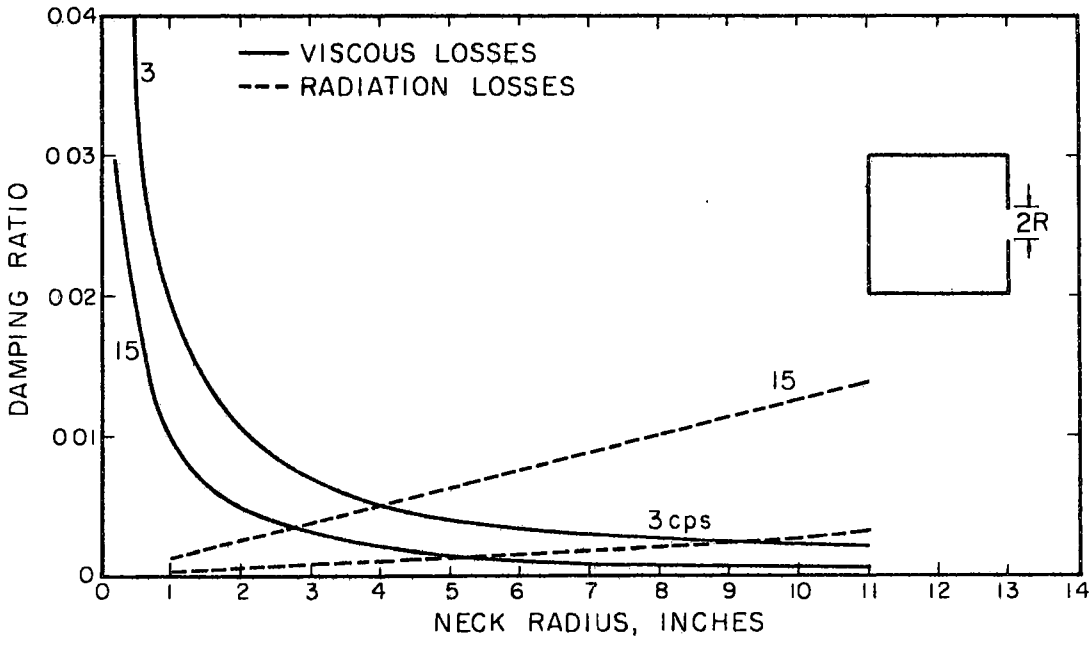

Comparison of Viscous and Radiation Losses

Figure 7. Theoretical Damping Ratio of Resonators

of the trace was necessary. The pressure oscillations inside the cavity were measured by a crystal microphone. The damping ratio was calculated using the standard log decrement technique. The block diagram of instrumentation is illustrated in Figure 8.

Experimental Results

The logarithmic decrements of resonators with necks of diameter 1.22" and 2.9" agree very well with the theoretical values for all lengths and volumes tested as indicated in Figures 9 and 10. The slight discrepancy can be attributed to the lack of accurate experimental technique to measure the damping. An error of even 10% could be made in counting the number of cycles. The l/d ratio of these necks were greater than or nearly equal to unity.

The experimental data for a 6.5" diameter neck differ considerably from the theoretical values (Figure 11). The measured damping ratios are much less than the calculated values. The l/d ratio of the necks tested were less than one. This means the end effects should have to be taken into account in the calculation of the damping ratio. Further the diameter of the neck was comparable to that of the resonator, the whole system behaved more like a pipe with a change in cross-section than a resonator with an orifice.

The measured natural frequencies for all combinations of neck areas, neck lengths and cavity volumes agree very well with the calculated values as shown in Figure 12. In general, the measured frequencies were less than the calculated undamped frequencies.

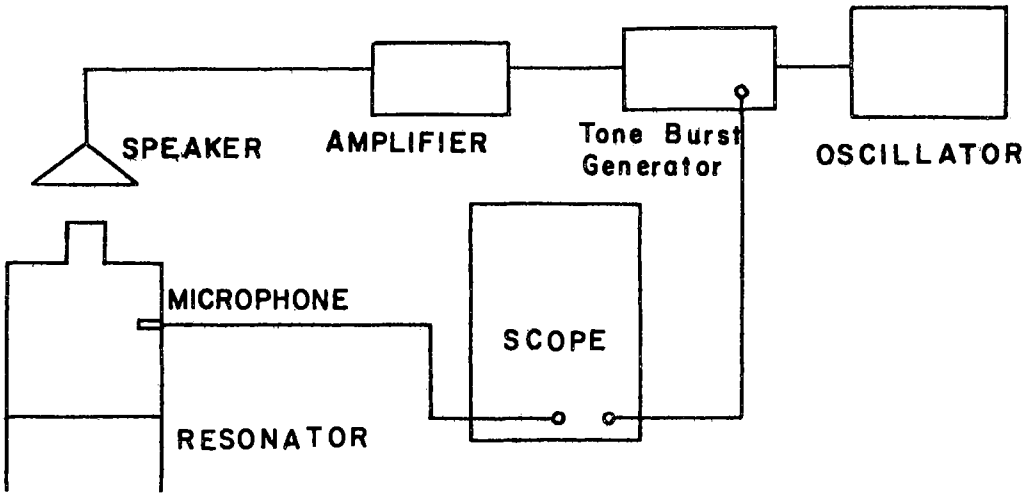

Figure 8. Experimental Set-Up for the Determination of Damping Ratios and Frequencies of Resonators

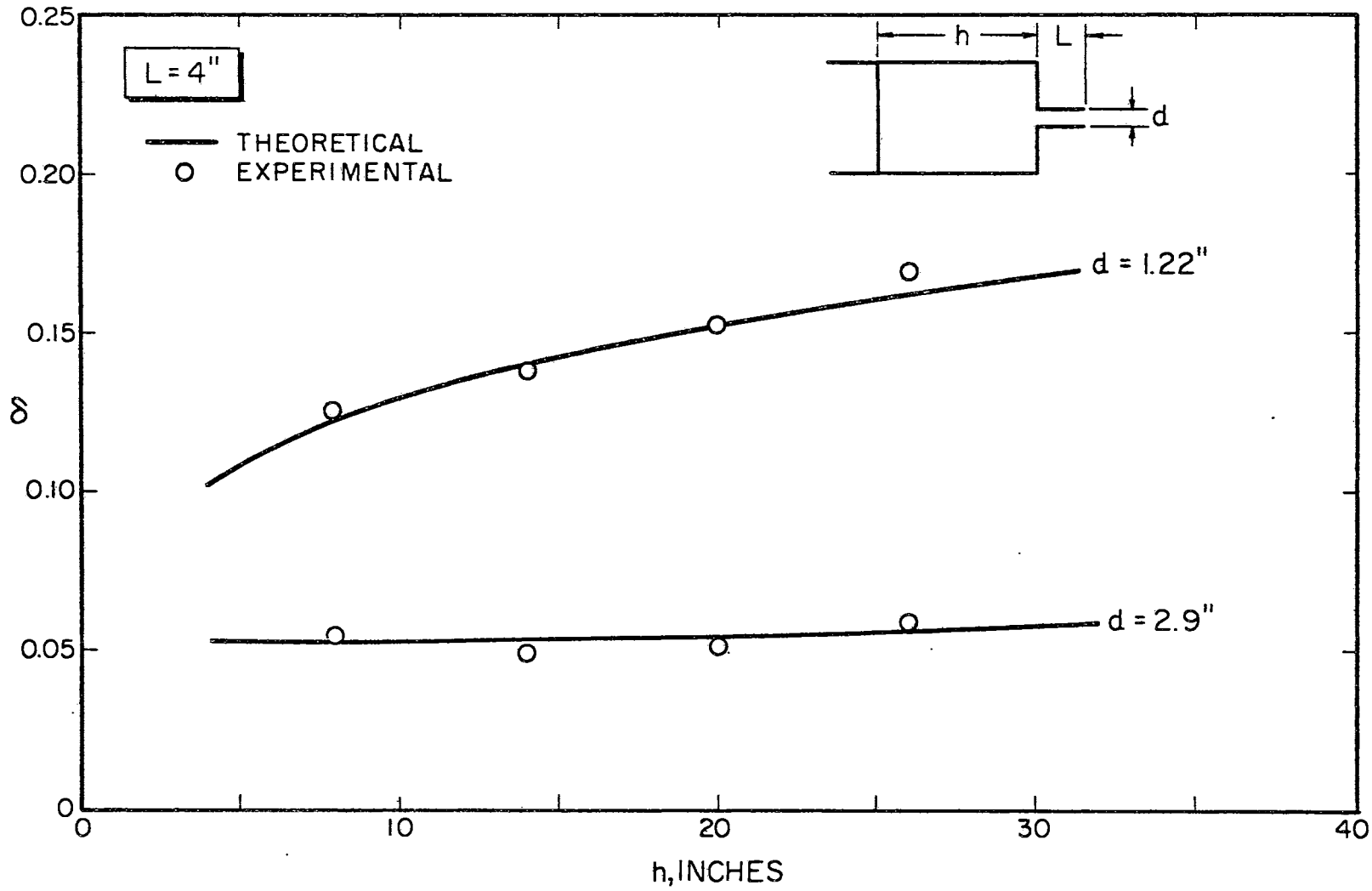

Figure 9. Logarithmic Decrement as a Function of Volume and Neck Size

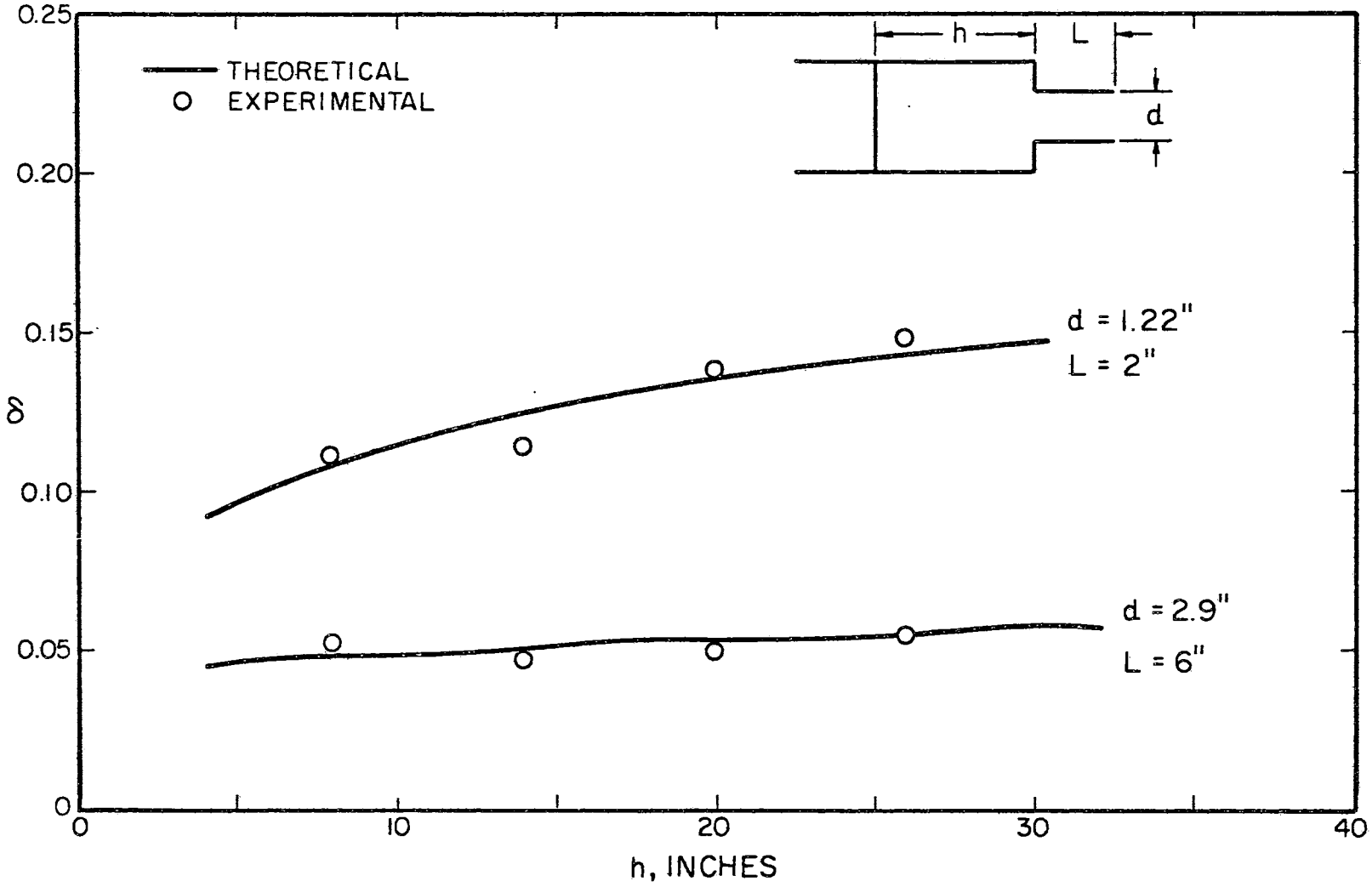

Figure 10. Logarithmic Decrement as a Function of Volume and Neck Size

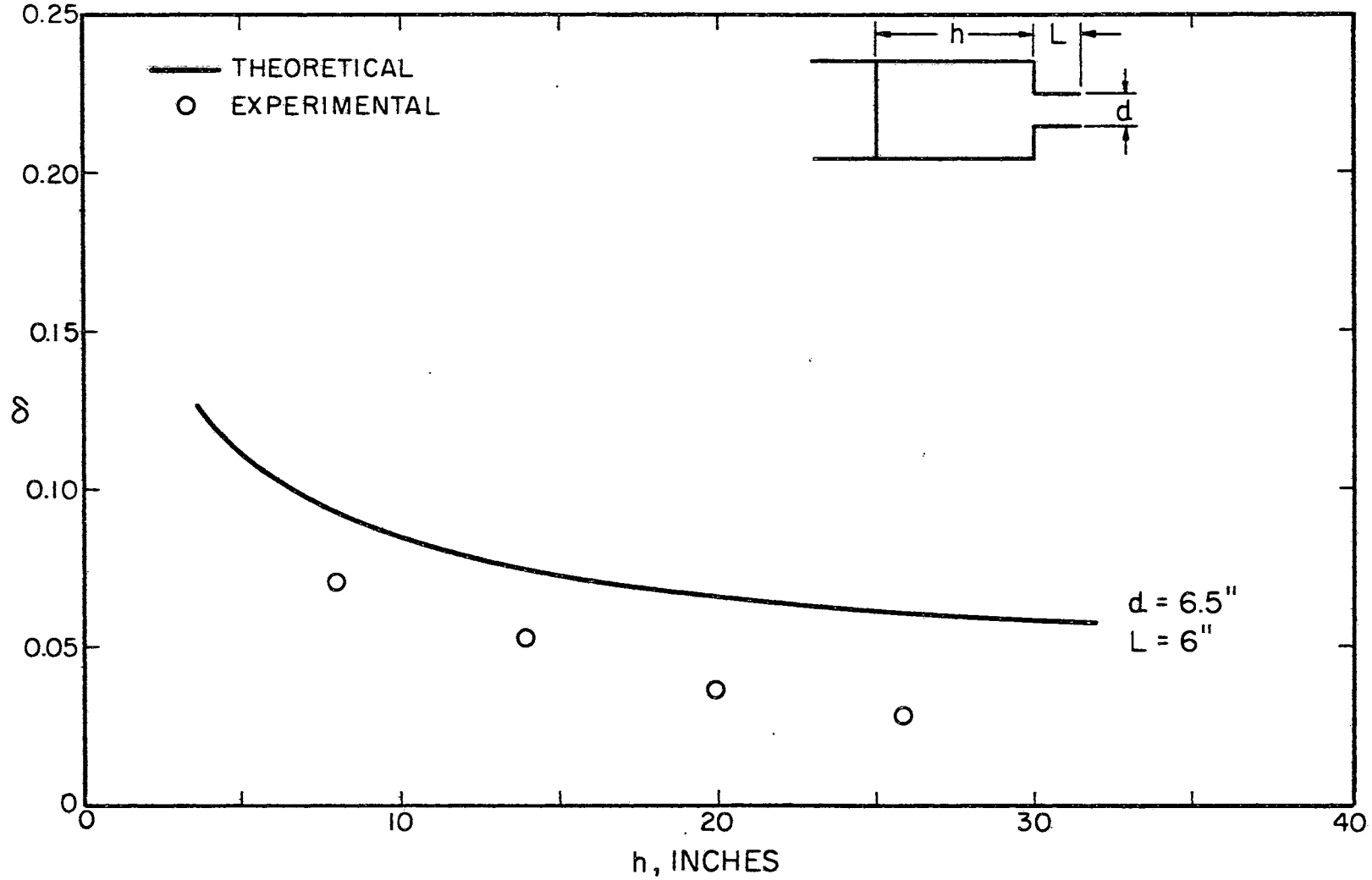

Figure 11. Logarithmic Decrement as a Function of Volume and Neck Size

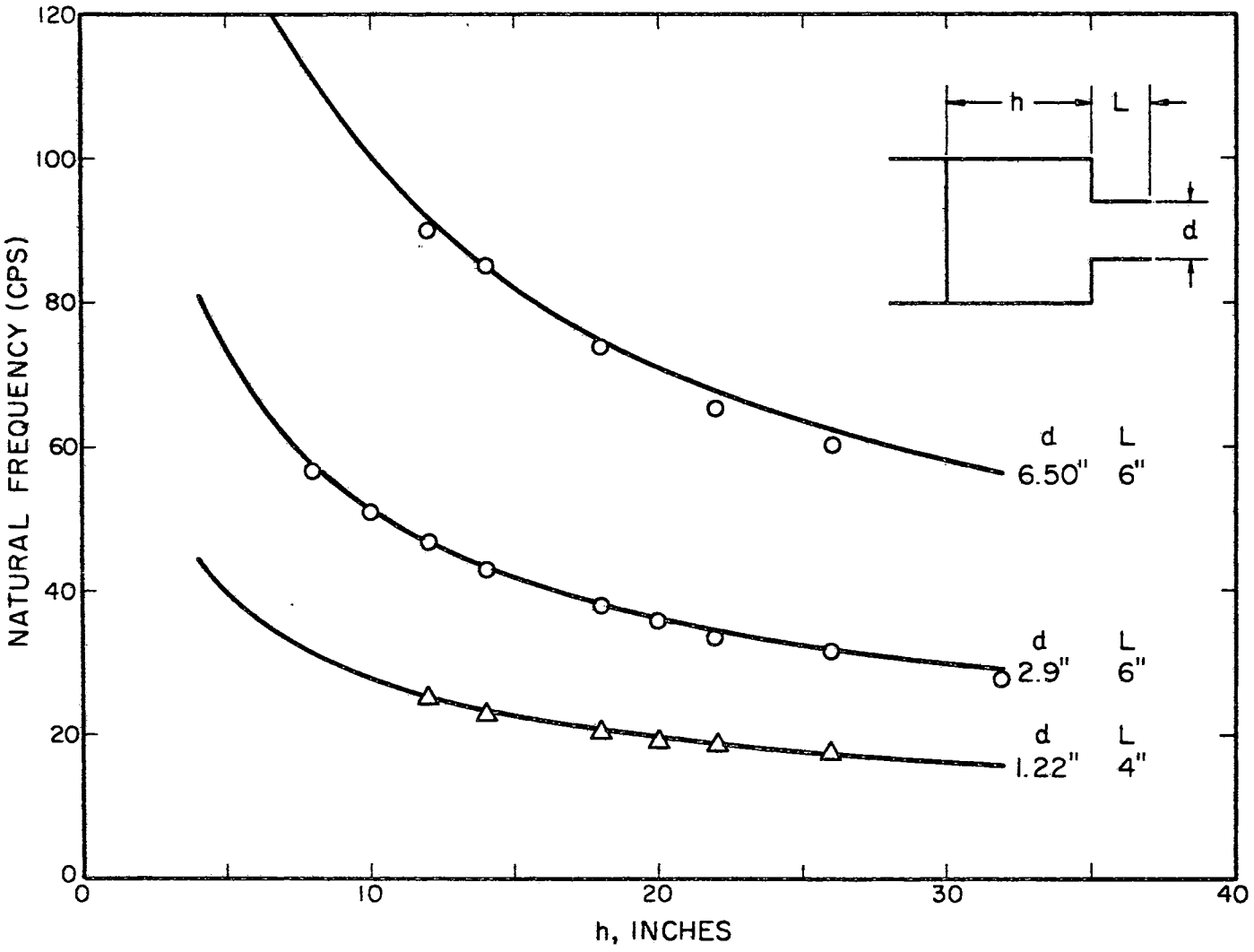

Figure 12. Experimental and Theoretical Natural Frequencies of Resonators

Other Observations

It was found that the damping was not linear whenever the input signal exceeded a certain limit. This limit was different for different combination of necks. The reason for this is when the input signal is increased the velocity of air in the neck is increased producing turbulence and jet effects (34). The net result is an increase in the viscous damping ratio and hence the total damping ratio. The reason could be either that there is a critical velocity or a critical Reynold's number above which the damping becomes non-linear.

From the response of the resonator for the pulse, the force at the neck can be found. The maximum velocity of air in the neck is $F/m\omega$ where,

F = Force

m = Mass of air in the neck

ω = Natural frequency in rps

A careful experiment was made on one combination of neck area, length, and cavity volume and the output signal above which the damping became non-linear was measured in terms of voltage. Assuming this value is theoretically correct, the critical voltage for all the other combinations of necks and cavities were calculated assuming (a) a constant critical Reynold's number and (b) a constant critical velocity. The results are as shown in Figures 13 and 14. Even though the results are not highly conclusive it can be said that the non-linearity in the damping is due to the fact that the velocity of the air in the neck exceeding a certain critical velocity rather than the Reynold's number exceeding a critical value. Hence it is possible to find the damping ratio for a larger pressure input by using a non-linear damping

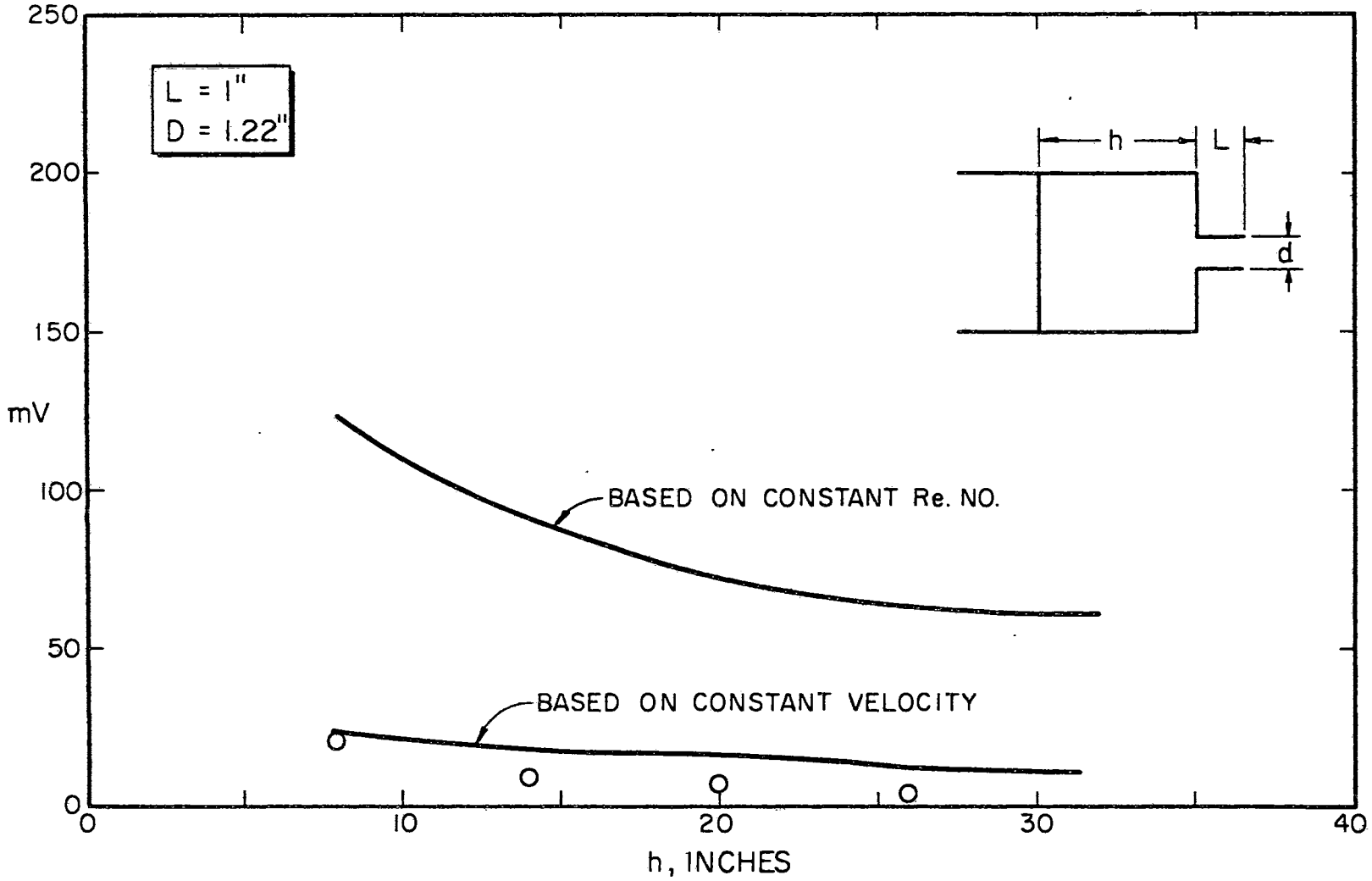

Figure 13. Critical Voltage as a Function of Volume and Neck Size

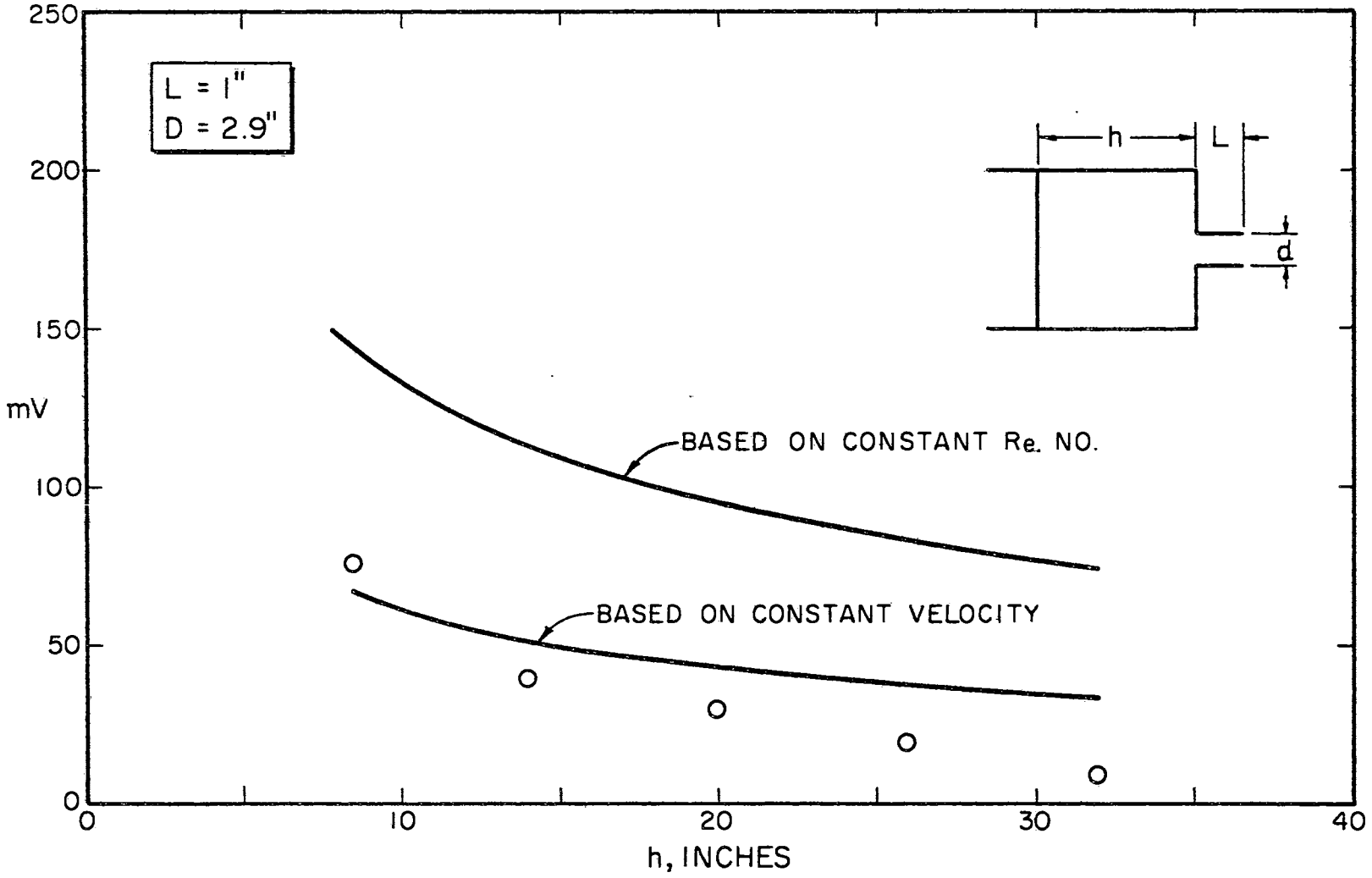

Figure 14. Critical Voltage as a Function of Volume and Neck Size

ratio which is a function of the velocity of the air in the neck.

$$\delta_{net} = \delta_{lin} + \delta_{n.l.} \tag{4-18}$$

$$\delta_{n.l.} \alpha (v - v_{cr})^n \tag{4-19}$$

The constant of proportionality and the index n can be found by a few accurate experimental results. But these values may differ considerably from resonator to resonator.

When the natural frequency of the resonator was about 130 cps a peculiar phenomena was observed. The trace in the oscilloscope clearly indicated pronounced beating. This beating was not due to the noise level in the room which is concentrated around 120 cps, because when the experiment was conducted outside the room which had the same noise level, no beats were observed. Further, in the same room the beats were found to depend upon the position of the resonator being predominate at quarter points and almost absent at the center of the room. This indicates that the standing waves in the room might have caused those beats. The frequency of the 202 mode for the room was 136 cps. Since the room was nearly square (16'x15'x9') it is quite likely that several modes have the frequency near 130 cps and the room responds strongly to the impressed sounds which are in the immediate vicinity of 130 cps. The continuous vortex shedding which causes the natural modes to break cannot be attributed to the beats because no pipe-tone was audible (34). The experiment has therefore to be conducted in a room with a different size or in an anechoic chamber to determine whether the standing waves are really the cause of the beats.

Damping Mechanisms in the Panel

The losses in the panel are due to

1. acoustic radiation damping
2. structural damping
3. other losses such as joint friction damping and support damping.

Acoustic Radiation Damping

The acoustic damping results from the reaction forces of the surrounding fluid on the radiating surfaces of a structure as energy is transferred from the radiator into the fluid. (20)

From (4-13) the resistive component of the acoustic impedance of a vibrating piston in an infinite baffle is

$$\frac{p}{U} = \frac{\rho_o c k^2}{2\pi} \tag{4-20}$$

For a uniform damping pressure,

$$p = \frac{\rho_o c k^2}{2\pi} \int_{J_o}^{b} \int_{J_o}^{a} u\,(x,y)\,dx\,dy \tag{4-21}$$

The velocity can be expressed in terms of the generalized coordinate q

$$p = \frac{\rho_o c k^2}{2\pi} \int_{J_o}^{a} \int_{J_o}^{b} \dot{q}\,\varphi\,(x,y)\,dx\,dy \tag{4-22}$$

where φ is the panel mode function.

The damping force can be obtained by integrating over the area of the panel which results in a damping factor

$$C = \frac{\rho_o c k^2}{2\pi} \left[\int_{J_o}^{b} \int_{J_o}^{a} \varphi\,(x,y)\,dx\,dy \right]^2 \tag{4-23}$$

The corresponding damping ratio is,

$$\zeta = \frac{\rho_o \omega}{4\pi cm} \left[\frac{\left\{ \int_o^b \int_o^a \Phi\,(x,y)\, dx\, dy \right\}^2}{\int_o^b \int_o^a \Phi^2\,(x,y)\, dx\, dy} \right] \qquad (4\text{-}24)$$

where m is the mass of the panel per unit area.

Once the modal function is known the contribution of the various modes to the damping ratio can be obtained from (4-24). For a simply supported panel vibrating in its fundamental mode ζ is given by,

$$\zeta = 3.684 \times 10^{-6} \frac{\rho_o}{\rho_m} \sqrt{\frac{E}{\rho_m}} \left(\frac{a}{b} + \frac{b}{a}\right) \qquad (4\text{-}25)$$

where ρ_o = density (mass/volume) of surrounding fluid and

ρ_m = density (mass/volume) of the panel material.

For glass panels vibrating in air this reduces to

$$\zeta = 0{\cdot}004618 \left(N + \frac{1}{N}\right) \qquad (4\text{-}26)$$

where N is the panel aspect ratio.

This theory predicts that for a given panel the damping ratio is a function only of the density of the panel and of the surrounding medium and not of the thickness. The damping ratio of glass panels for various a/b ratios is plotted in Figure 15. The square panel has the least damping.

Structural Damping

The behavior of elastic bodies subjected to stress is generally assumed to be ideal. The deflection of the panel is proportional to

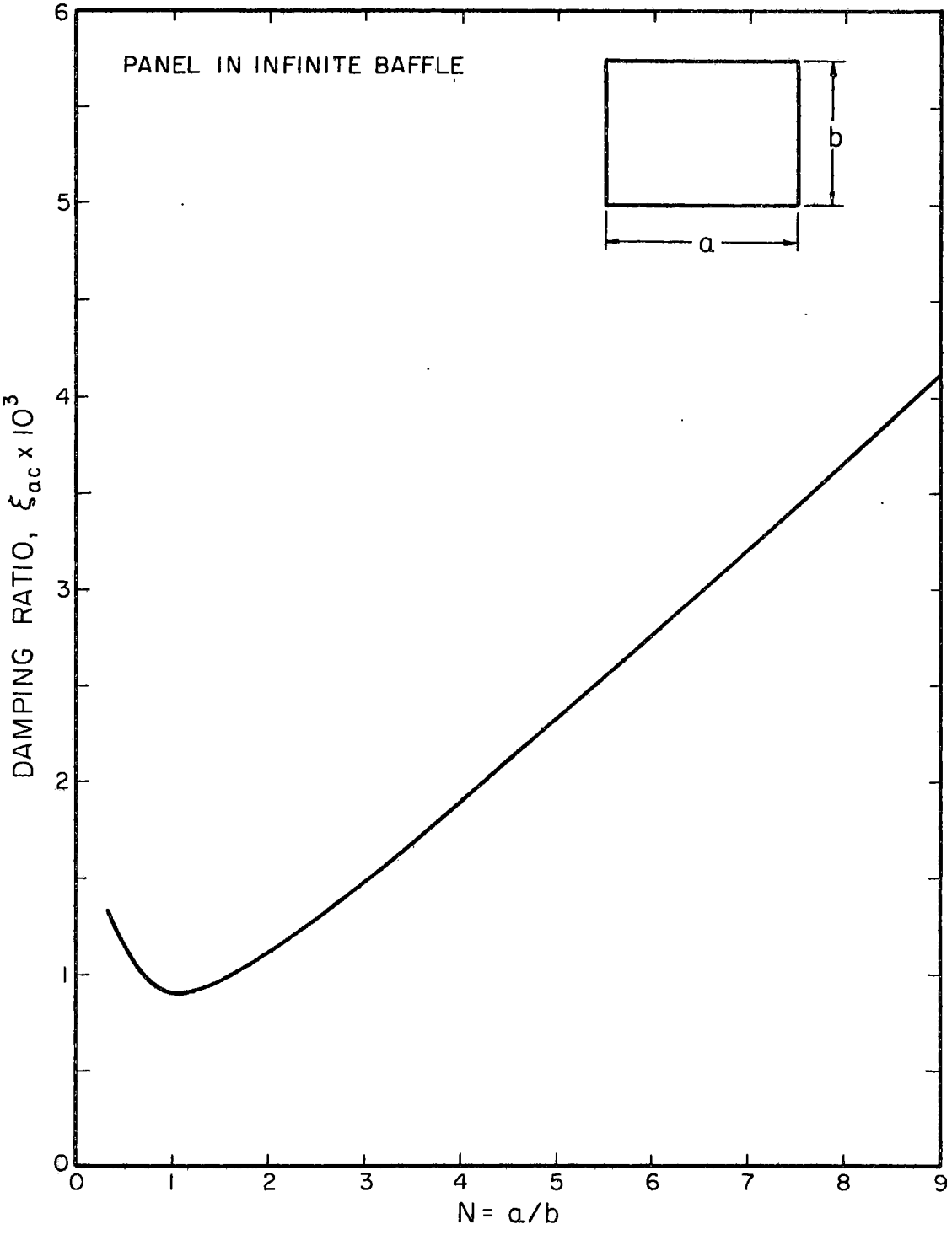

Figure 15. Acoustic Radiation Damping Ratio of Glass Panels

the applied load and when the load is removed the panel returns to its original position. But in practical situations this is not true because of the internal friction of the material. If the material is loaded over a cycle, the resulting load-deflection diagram will be as shown in Figure 16 instead of the linear relation for an ideal case. The area of the hysteresis loop represents the amount of internal friction or energy dissipated over a cycle of loading. For a vibrating body this represents the energy dissipated per cycle. The shape of the hysteresis loop depends on the loading and the material. In general the dissipated energy can be written as

$$D = k \sigma^{n} \tag{4-27}$$

where k = constant of proportionality

σ = the stress.

Only for the case of $n = 2$, is the damping linear and the response equations are therefore linear. For other values of n, to reduce the non-linear equations to linear equations, an equivalent viscous damping ratio has to be found keeping the damping energies the same.

It is rather difficult to measure the material damping of plate glass. Orloski (25) measured the decay rate of a vibrating Pyrex rod and arrived at a material damping ratio of 0.026. This can be taken as the representative figure for the plate glass as the damping mechanism is the same in both the cases.

System Damping

This involves the energy dissipated in various types of joints, interfaces or fasteners. The complexity of these increases due to the fact that the operating mechanism is coulomb friction. Therefore for

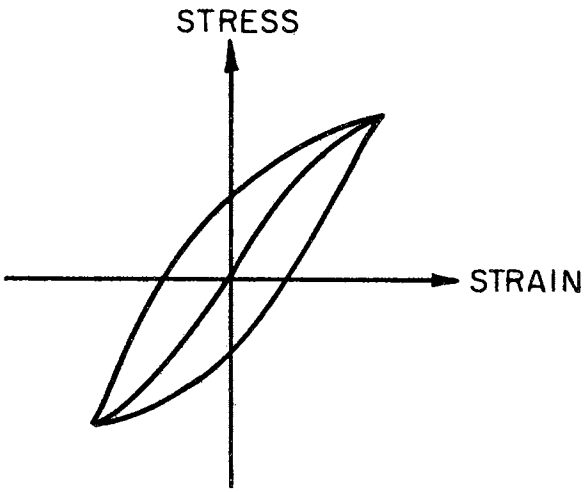

Figure 16. Hysteresis Loop or the Stress-Strain Curve for Repeated Loading

the damping ratio of plate glass panels it is necessary to rely on the experimental values.

Orloski (25) measured the damping ratios of several plate glass windows in the downtown stores of Stillwater. The panel was excited manually and the oscillations were picked up by a sensitive microphone and recorded using a pen-recorder. The damping ratio was obtained using the logarithmic decrement. He obtained a range of values from 0.01-0.05 for the damping ratio. The contribution to the damping by radiation damping is only a fraction of the total damping. The main damping mechanisms are the structural and joint friction damping. A representative figure of 0.03 can be taken for the regular size plate glass windows.

Knowing the damping ratios at the neck and in the panel the acoustic system is completely represented by its mathematical analog.

The transient response of such mathematical models is studied in the following chapters.

CHAPTER V

TRANSIENT RESPONSE OF MULTI-DEGREE OF FREEDOM SYSTEMS

The methods outlined in Chapter III on "Modeling" can be used to reduce any complicated physical system to an appropriate discrete system depending on the nature of the problem. The discrete system is represented by a number of second order ordinary simultaneous differential equations usually equal to the number of degrees of freedom. The response of the physical systems can be predicted from the results of the response analysis of single and multi-degree of freedom systems.

Undamped cases are initially studied so as not to lose the importance of various parameters in the total response. It is well known that for a single degree of freedom system for a steady sinusoidal load the amplitude approaches infinity when the frequency of excitation equals the natural frequency. But it can be shown that the maximax response for a cycle of sine pulse is finite and is equal to π. In fact this maximax response is a function of the number of cycles of loading and approaches infinity for the steady sinusoidal load. But for a sonic boom type of loading only one cycle of sine pulse need be analyzed. For an N-wave (Figure 17) excitation this maximax response can be shown to be less than π and equal to 2.16. (32) This is because an N-wave contains less impulse than the sine pulse of the same maximum amplitude.

Some acoustical systems can be represented as single degree of freedom systems. In all these cases the maximax response never exceeds 2.16 for sonic boom input. In fact the response will be less because of the inherent damping in the system as indicated in Chapter IV.

Most of the acoustical networks are not that simple. Even a room with a window and open door constitutes a two degree of freedom system. The hallways and various rooms in a structure give rise to additional degrees of freedom.

Transient Response of a Two Degree of Freedom System

In the case of a single degree of freedom system it is rather simple to express the maximax response as there is only one variable, the displacement, once the system natural frequency is fixed. But with two degrees of freedom the method is not as simple since the number of factors involved is greater, such as the uncoupled frequencies, coupled frequencies and coupling frequency. A general analysis is therefore not possible. The response can be found only for some particular cases. Further the response analysis has to be carried out for different loading conditions because the masses can be loaded according to the mode shapes or a combination of them.

Semi-Definite System

Figure 18 represents a two degree of freedom semi-definite system. A room with two opposite doors open corresponds to this system. The first mode gives zero change in volume and hence zero pressure magnification. It can be shown that for equal and opposite sinusoidal pulses on the masses the maximax response is always less

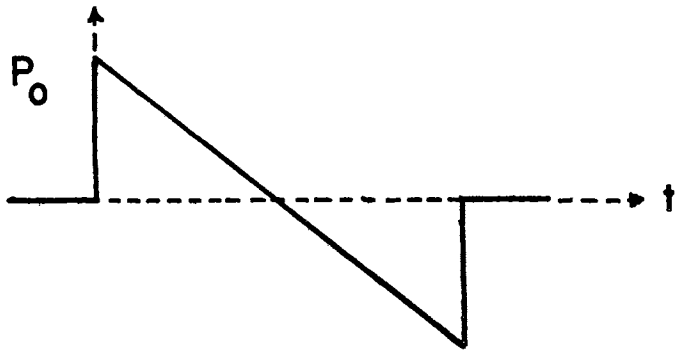

Figure 17. A Sonic Boom Signature

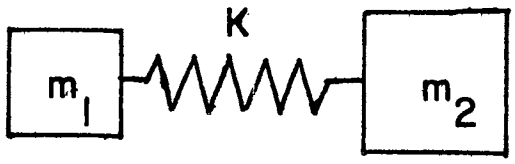

Figure 18. A Two Degree of Freedom Semi-Definite System

than π and approaches it when the mass ratio is very large

A two degree of freedom cantilever system is shown in Figure 29. The equations of motion of the above system can be solved using the Laplace transform. The solution in the complex $j\omega$ plane for forces $F_1(t)$ and $F_2(t)$ on the masses is given by,

$$X_1(s) = \frac{F_1(s)\left[s^2 + p_2^2\,(1 + F_2/F_1)\right]}{m_1\,(s^2 + p_+^2)\,(s^2 + p_-^2)} \qquad (5\text{-}1)$$

$$X_2(s) = \frac{F_2(s)\left[s^2 + p_{21}^2\,(1 + F_1/F_2) + p_1^2\right]}{m_2\,(s^2 + p_+^2)\,(s^2 + p_-^2)} \qquad (5\text{-}2)$$

where $F_1(s)$ and $F_2(s)$ = the corresponding transforms

p_1 and p_2 = uncoupled natural frequencies

p_+ and p_- = coupled natural frequencies and

p_{21} = coupling frequency

Once $F_1(s)$ and $F_2(s)$ are known the expressions for $X_1(s)$ and $X_2(s)$ can be reduced to partial fractions and retransformed to give a closed form solution. The response at any value of time is obtained using the computer. Table II gives the maximax response of a two degree of freedom cantilever system with identical masses and springs for an impulse and a step input. XX1 and XX2 are the non-dimensionalized responses, that is

$$XX1 = X_1/X_{st1} \text{ and} \qquad (5\text{-}3)$$

$$XX2 = X_2/X_{st2} \qquad (5\text{-}4)$$

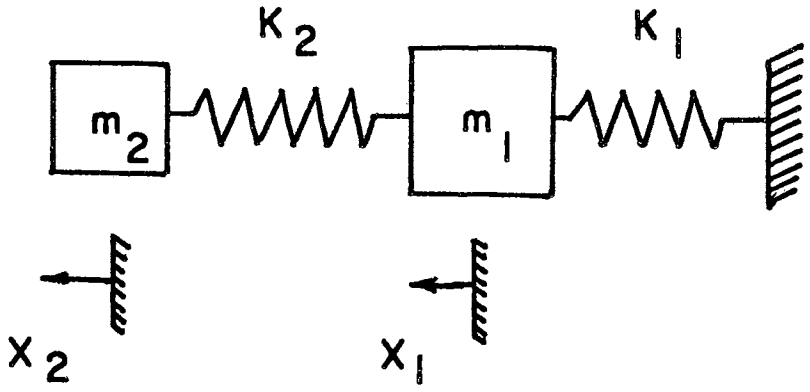

Figure 19. A Two Degree of Freedom Cantilever System

TABLE II

MAXIMAX RESPONSE OF A TWO DEGREE OF FREEDOM SYSTEM FOR IMPULSE AND STEP INPUT

Loads According to	Pulse Shape	XX1	XX2
First mode	Impulse	2.20	1.54
Second mode	Impulse	0.95	0.50
First mode	Step input	3.95	3.06
Second mode	Step input	1.62	0.97

The maximax response for a sinusoidal pulse as analyzed by the Laplace transformation method is not included in Table II. The reason for this is the sinusoidal pulse has a frequency term associated with it. When the forcing function frequency equals one of the two natural

frequencies of the system both the numerator and denominator of the expression for maximax response go to zero. Even though the solution obtained by Laplace transformation is in closed form, to evaluate the expression, increments of time have to be taken and thus the use of a computer is necessary. Due to the rounding off errors in the neighborhood of the critical frequency, maximax response as high as 100 were obtained which was definitely incorrect. The limit of the expression for the maximax response when the excitation frequency and the natural frequency are the same is found by using L'Hospital's rule. The response for sinusoidal loads can be found from (5-1) by substituting the corresponding values for $F_1(s)$ and $F_2(s)$.

$$XX1(t) = p_1^2\left[A\,\mathrm{Sin}\omega t + B\frac{\omega}{p_+}\,\mathrm{Sin}\,p_+t + \frac{C\omega}{p_-}\,\mathrm{Sin}\,p_-t\right] \quad \text{for } t<\tau \tag{5-5}$$

$$XX1(t) = p_1^2\left[A\left\{\mathrm{Sin}\omega t - \mathrm{Sin}\omega(t-\tau)\right\} + \frac{B\omega}{p_+}\left\{\mathrm{Sin}\,p_+t - \mathrm{Sin}\,p_+(t-\tau)\right\}\right.$$

$$\left. + \frac{C\omega}{p_-}\left\{\mathrm{Sin}\,p_-t - \mathrm{Sin}\,p_-(t-\tau)\right\}\right] \quad \text{for } t\geq\tau \tag{5-6}$$

where τ = the period of the pulse

$$A = -\left[\frac{\left\{p_+^2 - p_2^2\,(1 + F2/F1)\right\}}{(\omega^2 - p_+^2)\,(p_+^2 - p_-^2)} + \frac{\left\{(1 + F2/F1)p_2^2 - p_-^2\right\}}{(\omega^2 - p_-^2)\,(p_+^2 - p_-^2)}\right]$$

$$B = \frac{p_+^2 - p_2^2\,(1 + F2/F1)}{(p_+^2 - p_-^2)\,(\omega^2 - p_+^2)}$$

$$C = \frac{p_2^2\,(1 + F2/F1) - p_-^2}{(p_+^2 - p_-^2)\,(\omega^2 - p_-^2)}$$

From the results on the two degree of freedom system for rectangular pulse the maximum occurs at the end of the forced era or in the

residual era. The maximum of (5-6) will occur when the forcing function frequency equals one of the two natural frequencies, say p_-. Under this condition the response can be written as

$$XX1(t) = p_1^2 \left[\frac{B\omega}{p_+} \left\{ \text{Sin } p_+t - \text{Sin } p_+ (t-\tau) \right\} + \frac{C\omega}{p_-} \left\{ \text{Sin } p_-t - \text{Sin } p_-(t-\tau) \right\} \right] \qquad (5\text{-}7)$$

because the contribution by the first term in (5-6) is zero. The contribution by the third term is found by substituting the value for the constant C and letting $\omega = p_-$. This results in,

$$(XX1)_{Cmax} = \lim_{\alpha \to 1} \frac{2 \left[(1 + \frac{F2}{F1})\ p_+^2 - p_1^2 \right] \alpha \text{ Sin } \pi\alpha}{(1 - \alpha^2)\ (p_+^2 - p_-^2)} \qquad \text{--- (5-8)}$$

$$= \frac{\pi \left[(1 + \frac{F2}{F1})\ p_+^2 - p_1^2 \right]}{(p_+^2 - p_-^2)} \qquad (5\text{-}9)$$

The contribution to the response by the second term is very small compared to (5-9) and hence can be ignored. Similarly, if the excitation frequency ω equals p_+ the maximax response will be

$$XX1_{max} = \frac{\pi \left[p_1^2 - p_-^2\ (1 + F2/F1) \right]}{(p_+^2 - p_-^2)} \qquad \text{--- (5-10)}$$

Table VII gives the maximax response of a two degree of freedom cantilever system with identical springs and masses for sinusoidal pulse.

The above method of taking the limit as the excitation frequency equals one of the natural frequencies gives only the maximax response. To get the response as a function of time the two differential equations of motion were integrated numerically using Runge-Kutta-Adams-Moulton method. The response curves for the two different loading

cases are plotted in Figures 20 and 21. It is seen that the maximax response obtained using L'Hospital's rule agrees very well with the values calculated using numerical integration.

TABLE III

MAXIMAX RESPONSE OF A TWO DEGREE OF FREEDOM SYSTEM FOR SINUSOIDAL PULSE

F_1	F_2	Theoretical Maximax XX1		Theoretical Maximax XX2	
		$\omega = p_-$	$\omega = p_+$	$\omega = p_-$	$\omega = p_+$
1	1	6.05	0.31	4.80	0.10
1	-1	1.59	1.40	1.20	0.45
1	0	3.54	0.87	1.84	0.27
0	1	3.67	0.52	2.84	0.70

From these results it is clear that the maximax response of a two degree of freedom system is essentially a function of the difference in the natural frequencies of the system. The maximax approaches infinity as p_+ approaches p_-. Since in no physical system can this happen the maximax transient response of a two degree of freedom system is bounded. This again can be expected because the transient response of a single degree of freedom system is bounded. It can also be seen that the response is most severe when the loads are acting according to the first mode configuration. This is true for all pulse shapes.

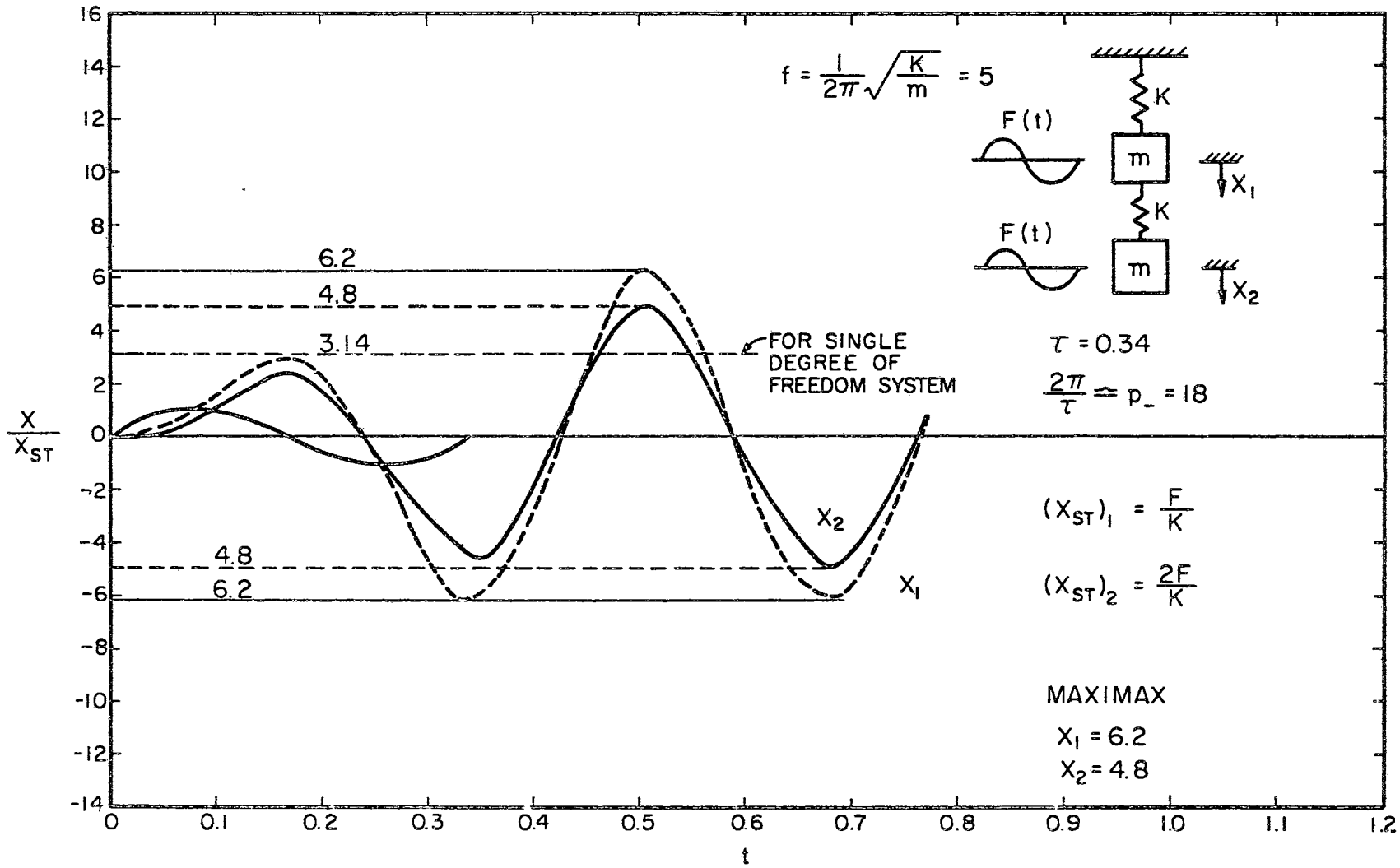

Figure 20. Non-Dimensional Response for a Two Degree of Freedom Cantilever System for Sinusoidal Pulse According to the First Mode

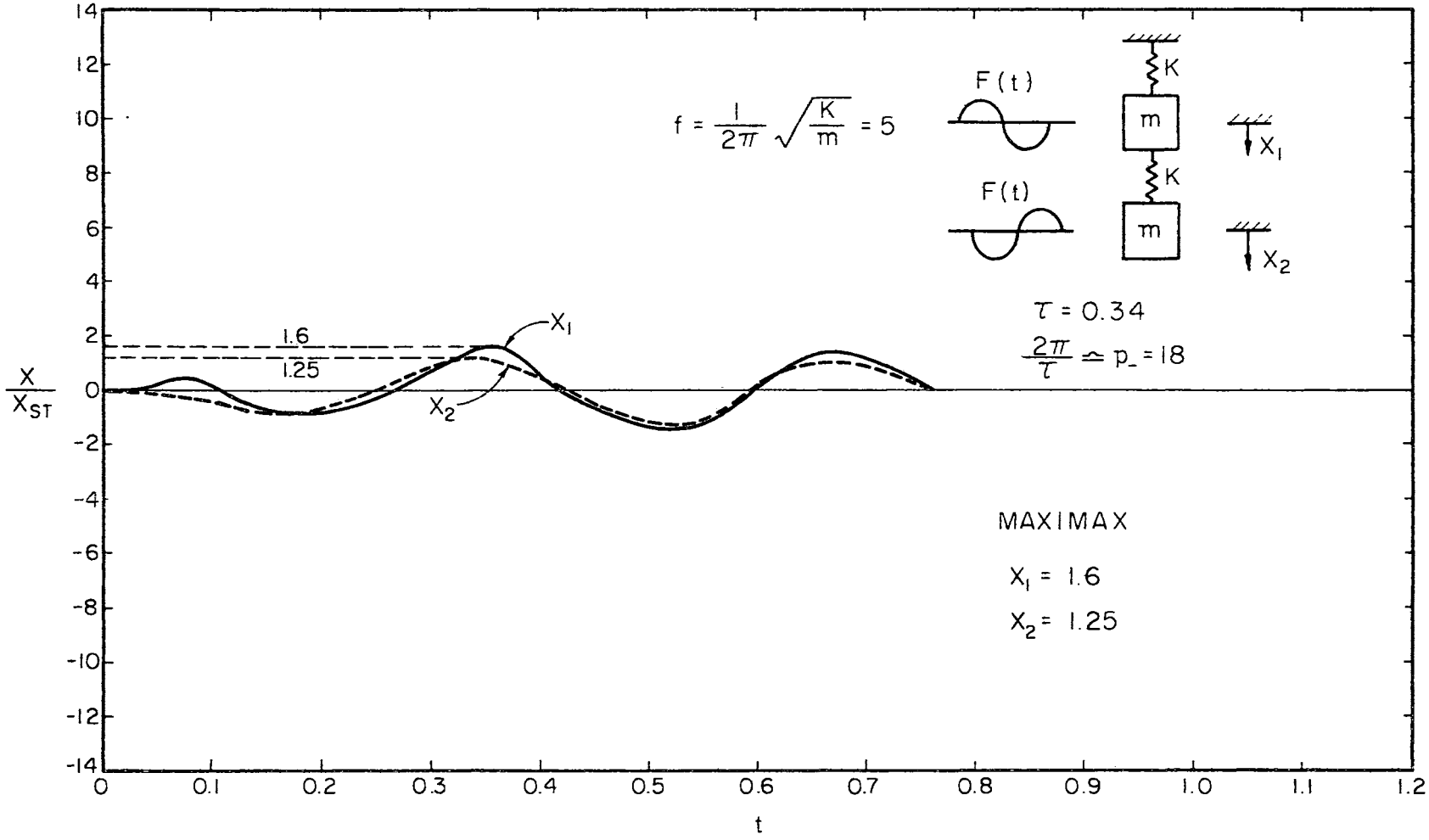

Figure 21. Non-Dimensional Response for a Two Degree of Freedom Cantilever System for Sinusoidal Pulse According to the Second Mode

Two Mass Three Springs System

A two degree of freedom symmetrical system in shown in Figure 22.

Using identically the same method outlined in the previous section the expression for the maximax response for sinusoidal pulse is found as,

$$XX1 = \frac{s_{11}\,(p_+^2 - p_1^2)\,\pi}{(p_+^2 - p_-^2)} \tag{5-11}$$

where

$$s_{11} = \frac{k_2 + k_3 + k_2\,k_3/k_1}{k_2 + k_3}$$

The maximax response for a system with identical masses and springs will be 5.14 when the loads are acting according to the first mode configuration which agrees with the value calculated using numerical integration. The response is less than that of a two degree of freedom cantilever system.

Three Degree of Freedom System

As mentioned earlier the complexity of analysis increases considerably with the number of degrees of freedom because of the many variables involved. An identical technique is used to find the maximax response for sinusoidal pulse.

The maximax response for sinusoidal pulse is given by,

$$XX1_{max} = \frac{\pi\left[p_b^2\,p_c^2\,(1 + \frac{F2}{F1} + \frac{F3}{F1}) - s_1\,p_1^2 - p_a^2\,p_1^2 + p_c^2\,p_1^2\right]}{(p_a^2 - p_b^2)\,(p_a^2 - p_c^2)} \tag{5-12}$$

where F_1, F_2, F_3 = maximum amplitude of the loads

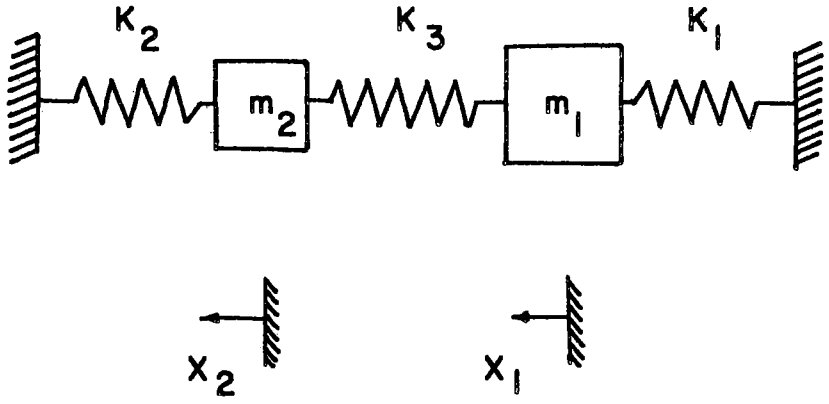

Figure 22. A Two Degree of Freedom Symmetrical System

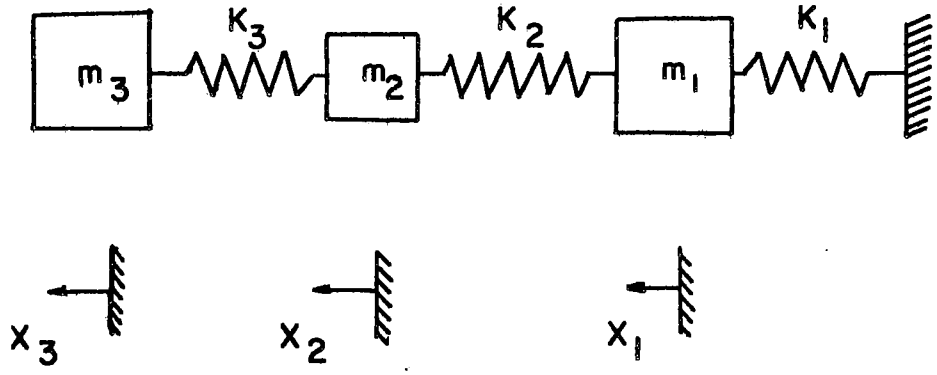

Figure 23. A Three Degree of Freedom Cantilever System

p_1, p_2, p_3 = uncoupled natural frequencies

p_a, p_b, p_c = coupled frequencies

$$s_1 = p_3^2 + p_2^2 \left(1 + \frac{F2}{F1}\right) + p_{32}^2$$

$$s_2 = p_2^2 \, p_3^2 \left(1 + \frac{F2}{F1} + \frac{F3}{F1}\right)$$

p_{32}, p_{31} = coupling frequencies

As in the two degree of freedom system it is found that the transient maximax response of a three degree of freedom system is limited only by the differences of the squares of the natural frequencies taken two at a time. Since in general the three natural frequencies are different the maximax response is limited. Figures 24 and 25 give the response curves for two different loading conditions. The values of maximax response 8.85 and 2.34 agree well with the values calculated using L'Hospital's rule. Once again the response is most severe when the loads are acting according to the first mode configuration.

Infinite Degrees of Freedom System

As seen before, the complexity of the problem increases with the number of degrees of freedom. But when the number of masses is really large, the system can be considered to be an infinite degree of freedom system. The system therefore approaches the longitudinal vibrations of a rod which can be represented by a single linear partial differential equation.

The equation of motion for the longitudinal vibrations of a rod is

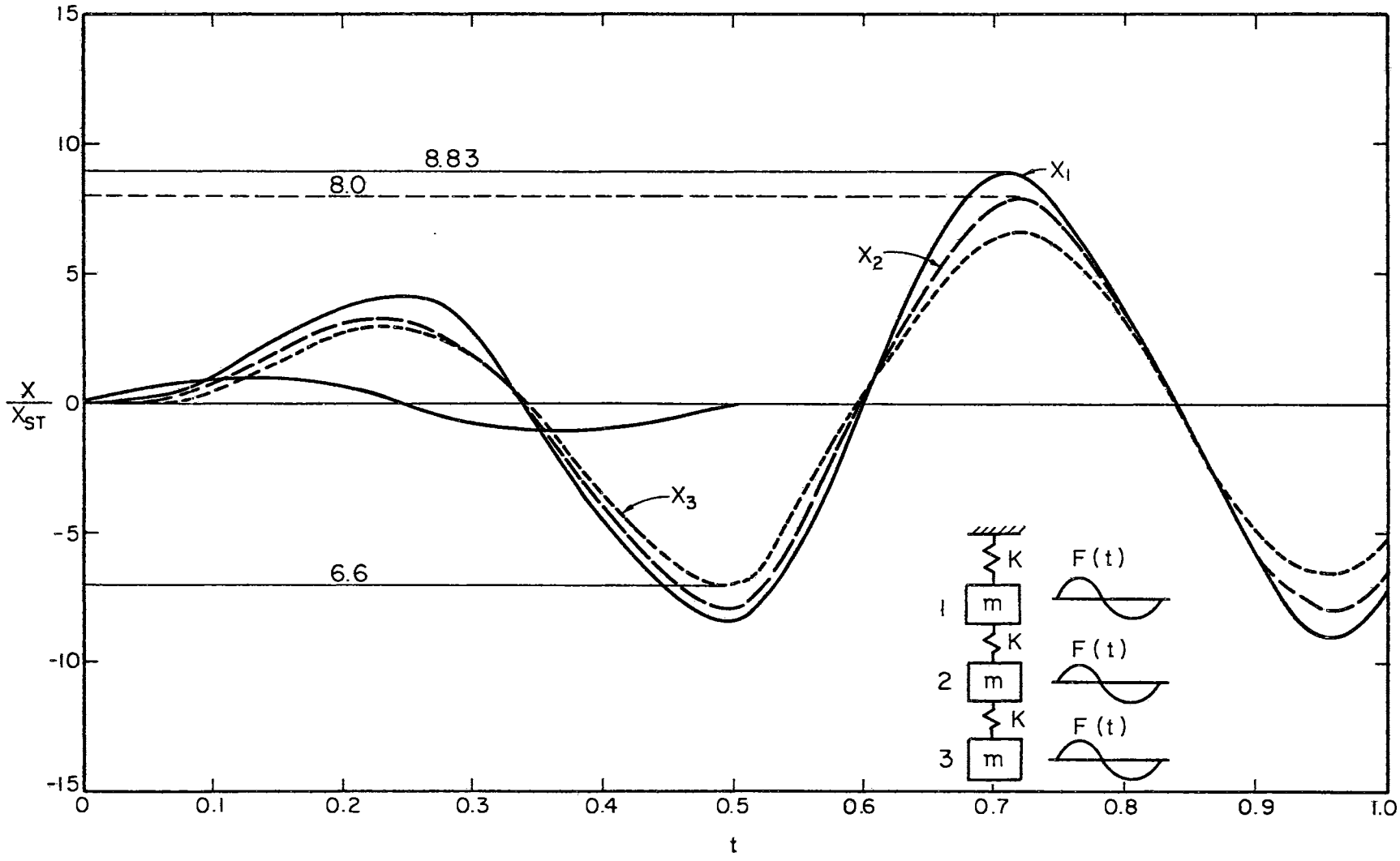

Figure 24. Non-Dimensional Response for a Three Degree of Freedom Cantilever System for Sinusoidal Pulse According to the First Mode

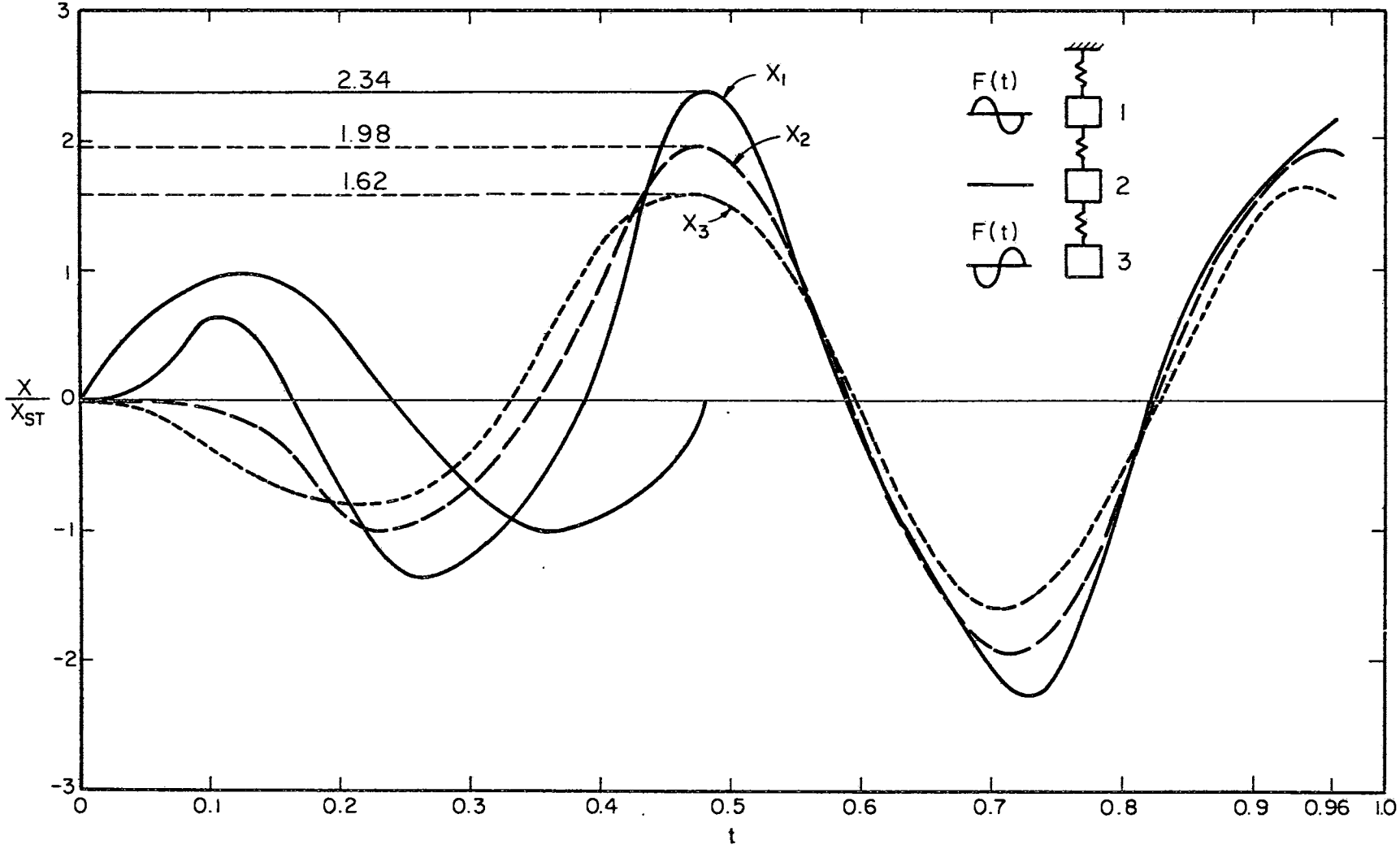

Figure 25. Non-Dimensional Response for a Three Degree of Freedom Cantilever System for Sinusoidal Pulse According to the Second Mode

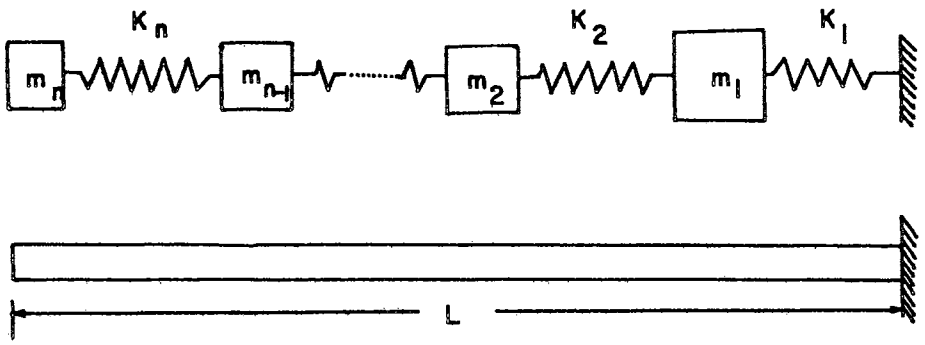

Figure 26. Infinite Degree of Freedom System

$$\frac{\partial^2 u}{\partial t^2} = \frac{E}{\mu}\frac{\partial^2 u}{\partial x^2}\frac{1}{A\mu} f(x,t) \qquad (5\text{-}13)$$

where μ = mass density of the material of the bar.

The natural frequencies can be obtained by letting f(x,t) = 0 and solving the corresponding linear equation. For a bar of length L built-in at one end and free at the other, the natural frequencies are given by,

$$\omega_n = \frac{\pi \alpha n}{2L} \qquad \text{where} \quad \alpha = \sqrt{\frac{E}{\mu}} \qquad (5\text{-}14)$$

The solution to the equation of motion can be written as (37),

$$u(x,t) = \sum_{m=1,3,5\cdots}^{\infty} q_m(t) \sin\frac{m\pi x}{2L} \qquad (5\text{-}15)$$

where q_m = the generalized co-ordinate.

The expression for q_m can be obtained using the principle of virtual work.

$$q_m = (-1)^{(m-1)/2} \cdot \frac{4\alpha}{AE\pi m} \int_0^t F(\tau) \sin\frac{m\pi\alpha}{2L}(t-\tau)d\tau \qquad (5\text{-}16)$$

where $F(\tau)$ is the forcing function applied at the free end.

Response for a Step Input at x = L

For a step input

$$F(\tau) = F_o \text{ for } t > 0 \tag{5-17}$$

The solution for u(x,t) is obtained by substituting (5-17) in (5-16) and performing the indicated integration.

$$u(x,t) = \sum_{m=1,3,5---}^{\infty} (-1)^{(m-1)/2} \cdot \frac{8F_o L}{EAm^2\pi^2} \left[1 - \text{Cos} \frac{m\pi\alpha t}{2L}\right] \text{Sin} \frac{m\pi x}{2L} \tag{5-18}$$

The maximum displacement occurs at x = L.

$$u(L,t) = \sum_{m=1,3,5---}^{\infty} (-1)^{(m-1)/2} \cdot \frac{8F_o L}{EAm^2\pi^2} \left[1 - \text{Cos} \frac{m\pi\alpha t}{2L}\right] \tag{5-19}$$

When $t = 2\alpha$,

$$u(L,t)_{max} = \frac{16F_o L}{AE\pi^2} \sum_{1,3,5--}^{\infty} \frac{1}{m^2} = \frac{2F_o L}{AE} \tag{5-20}$$

The maximax response for a step input is therefore 2.0 which is the same as for a single degree of freedom system.

Sinusoidal Load at x = L

The non-dimensional maximax response at x = L for a sinusoidal load can be found similarly. The expression for the response is,

$$U(L,t) = \sum_{m=1,3,5--}^{\infty} \frac{8\omega_m}{\pi^2 m^2} \left[\frac{\omega \text{Sin}\omega_m t - \omega_m \text{Sin}\omega t}{(\omega^2 - \omega_m^2)}\right] \tag{5-21}$$

The response for a cycle of sinusoidal pulse can be obtained by the principle of superposition as,

$$U(L,t) = \sum_{m=1,3,5--}^{\infty} \frac{8\omega_m}{\tau^2 m^2(\omega^2-\omega_m^2)} \left[\omega\left\{\mathrm{Sin}\omega_m t - \mathrm{Sin}\omega_m(t-\tau)\right\} - \omega_m\left\{\mathrm{Sin}\omega t - \mathrm{Sin}\omega(t-\tau)\right\}\right] \qquad (5\text{-}22)$$

This reduces to the form given in (5-23) because $\omega\tau = 2\pi$.

$$U(L,t) = \sum_{m=1,3,5--}^{\infty} \frac{8\omega_m}{m^2\pi^2} \frac{1}{(\omega^2-\omega_m^2)} \left\{\omega\mathrm{Sin}\omega_m t - \omega\mathrm{Sin}\omega_m(t-\tau)\right\} \qquad (5\text{-}23)$$

The maximum of (5-23) will occur when each of the terms in the series is a maximum. It is evident that all the terms cannot satisfy this condition because in no physical system can all the natural frequencies be the same. The upper bound of response can be found by assuming that all the natural frequencies have the same value. The response for this hypothetical case is

$$U_{max}(L,t) = \pi \qquad (5\text{-}24)$$

Therefore the response of an infinite degree of freedom system for a cycle of sinusoidal pulse at the free end can never exceed π which is also the maximax for a single degree of freedom system.

The above analysis was carried out for a load at the free end only. If there are additional load points which are not too close to the fixed end the maximax can be found by using the influence coefficients. The response for a number of load points is,

$$U = \pi\left[1 + \frac{n-1}{n} + \frac{n-2}{n} + \text{---}\right] \qquad (5\text{-}25)$$

where n is the number of degrees of freedom.

For example, the maximax response for a simultaneous sinusoidal pulse at the free end and at $x = L/2$ will be $3\pi/2$.

Single Degree of Freedom Non-Linear System

In the previous analysis the springs were assumed to be perfectly elastic and the response was obtained analytically and numerically. In actual systems the springs may exhibit a non-linear hard spring type load - deflection relationship. The equation of motion of a single degree of freedom hard spring system is

$$\ddot{x} + \omega_n^2 x + \epsilon x^3 = F(t) \qquad (5\text{-}26)$$

where ϵ is the non-linearity coefficient.

This equation was solved for an N-wave for zero initial conditions. Figure 27 shows the maximax response for different values of ϵ. It is seen that the maximax response reduces with increase in the non-linearity coefficient.

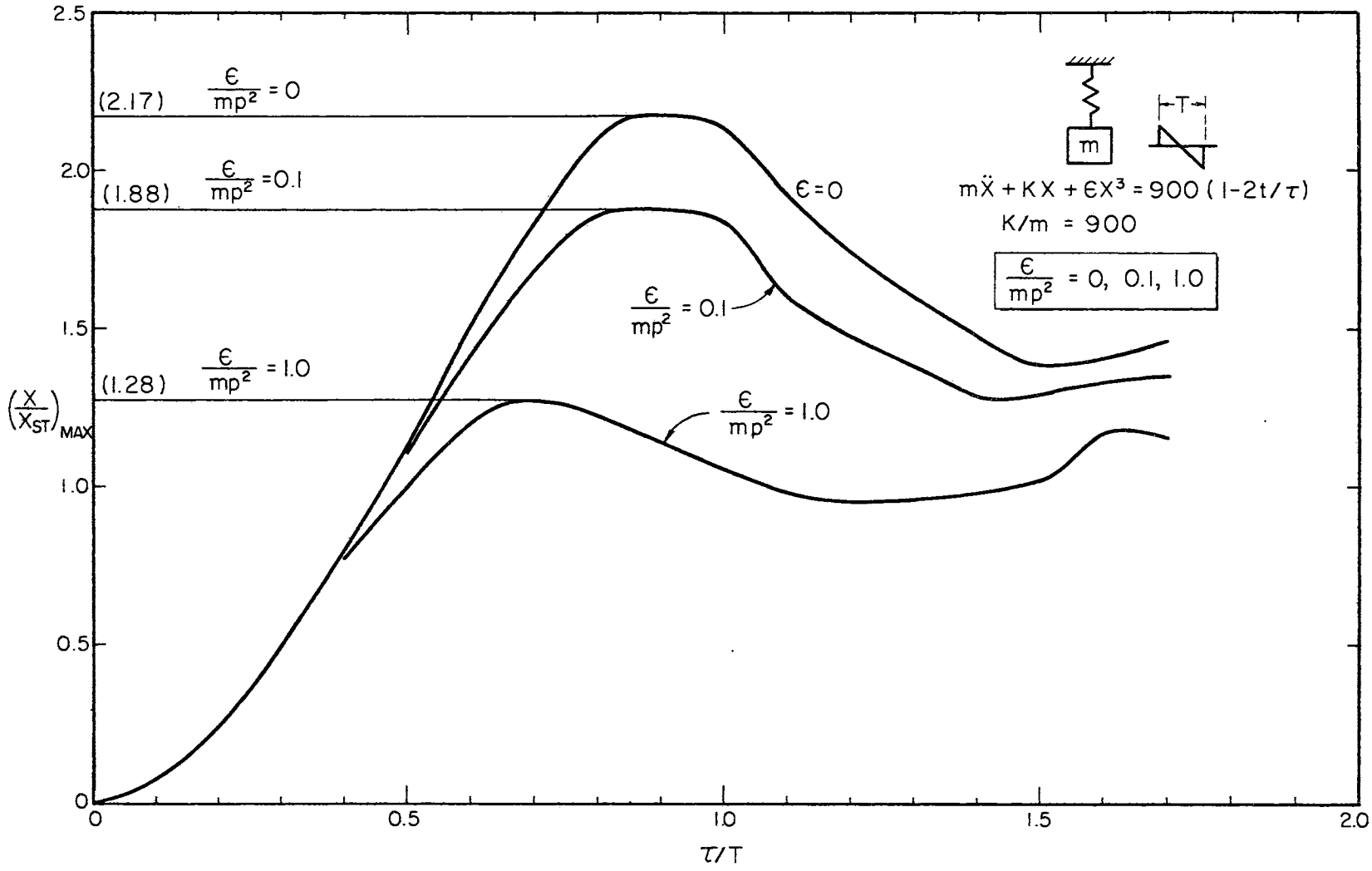

Figure 27. Maximax Response of a Simple Hard Spring System for N-Wave

CHAPTER VI

RESPONSE OF MECHANO-ACOUSTICAL NETWORKS TO TRANSIENT EXCITATION

In Chapter V, the transient response of several mechanical systems were discussed. In this chapter the response of acoustical networks represented by those models will be studied. Damping will be included because the systems to be treated here are realistic. The pressure magnifications in the cavities and the stress magnifications in the panels will be found for various types of buildings.

Stress and Strain in the Panel in Terms of Displacement

The panel is assumed to vibrate in its fundamental mode. Then,

$$w = w_o \text{ Sin } \pi x/a \text{ Sin } \pi y/b \tag{6-1}$$

If $a > b$, the maximum stresses at the center of the panel is (37),

$$\sigma_{max} = \frac{-6D}{h^2}\left[\frac{\upsilon}{a^2} + \frac{1}{b^2}\right]\pi^2 w_o \tag{6-2}$$

where D = flexural rigidity of the panel

h = thickness and

υ = Poisson's ratio

The corresponding maximum strain will be

$$e_{max} = \frac{-\pi^2 h w_o}{2b^2} \tag{6-3}$$

It was found in Chapter V that the response for a single degree of freedom system for a sonic boom load never exceeded 2.16. Hence mechano-acoustical systems which can be represented as single degree of freedom systems (Figure 28) are not critical to sonic boom.

Systems Having Two Degrees of Freedom

In the single degree of freedom system the maximum transient response is bounded. In a two degree of freedom system the maximax response is controlled by the natural frequencies of the system. Consequently higher pressure and stress magnifications can be expected in acoustical networks which are represented as multi degree of freedom systems. Figure 29 shows such types of systems. When a supersonic aircraft passes over the types of buildings represented in Figure 29 three different loading conditions are possible (Figure 30).

The expression for the maximax response of a two degree of freedom cantilever system for equal and opposite sinusoidal pulse on the masses is (5-10),

$$XX1 = \frac{\pi p_1^2}{(p_+^2 - p_-^2)} \tag{6-4}$$

For a given neck area, neck length, panel size the maximax response is plotted as a function of the cavity volume as shown in Figure 31. It has a maximum value of 10.23.

The expression for the maximax response of a two mass three spring system from (5-11) is,

$$XX1 = \frac{\pi(p_1^2 - p_1^2 p_2^2/p_+^2)}{(p_+^2 - p_-^2)} \tag{6-5}$$

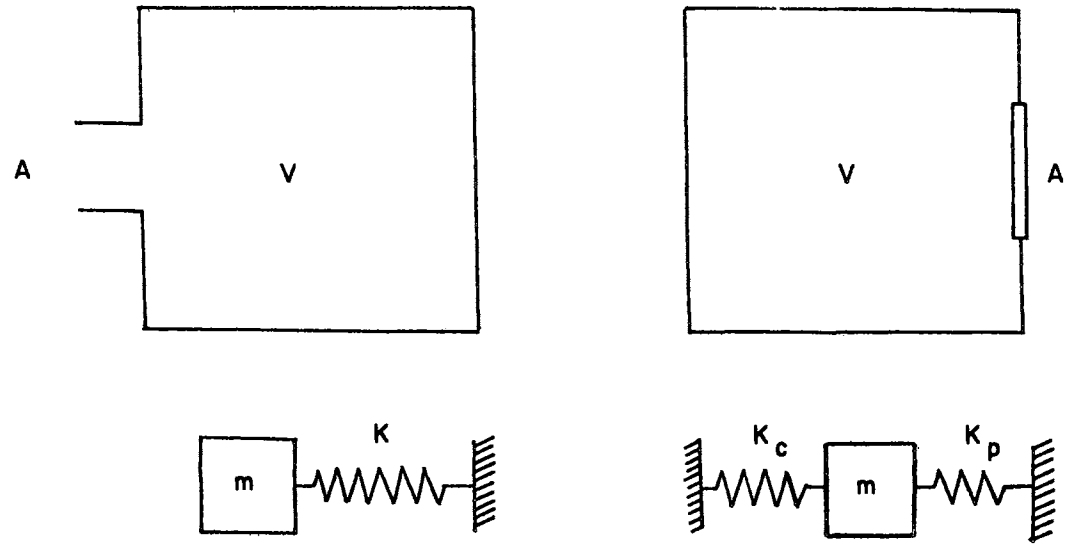

Figure 28. Networks Which Can Be Represented as Single Degree of Freedom Mechanical Systems

Figures 32 and 33 indicate this response as a function of the cavity volume for two different loading conditions. It is seen that the maximax response for a sonic boom type loading is always less than π and approaches this value when the volume is very large. Therefore for a large cavity volume the stiffness of the center spring is almost zero and the system degenerates into two separate single degree of freedom systems whose maximax response is π. (Figure 34)

From (6-4) and (6-5) it can be repeated again that closer the natural frequencies are, greater is the response. The frequencies will be closer if the mass ratio is large. Of the systems shown in Figure 29, (a), (b) and (d) have mass ratios unity or not much different from unity. Their natural frequencies are therefore farther apart. Systems (c) and (e) can have a large mass ratio because the density of air is much smaller compared to the density of the glass and hence the

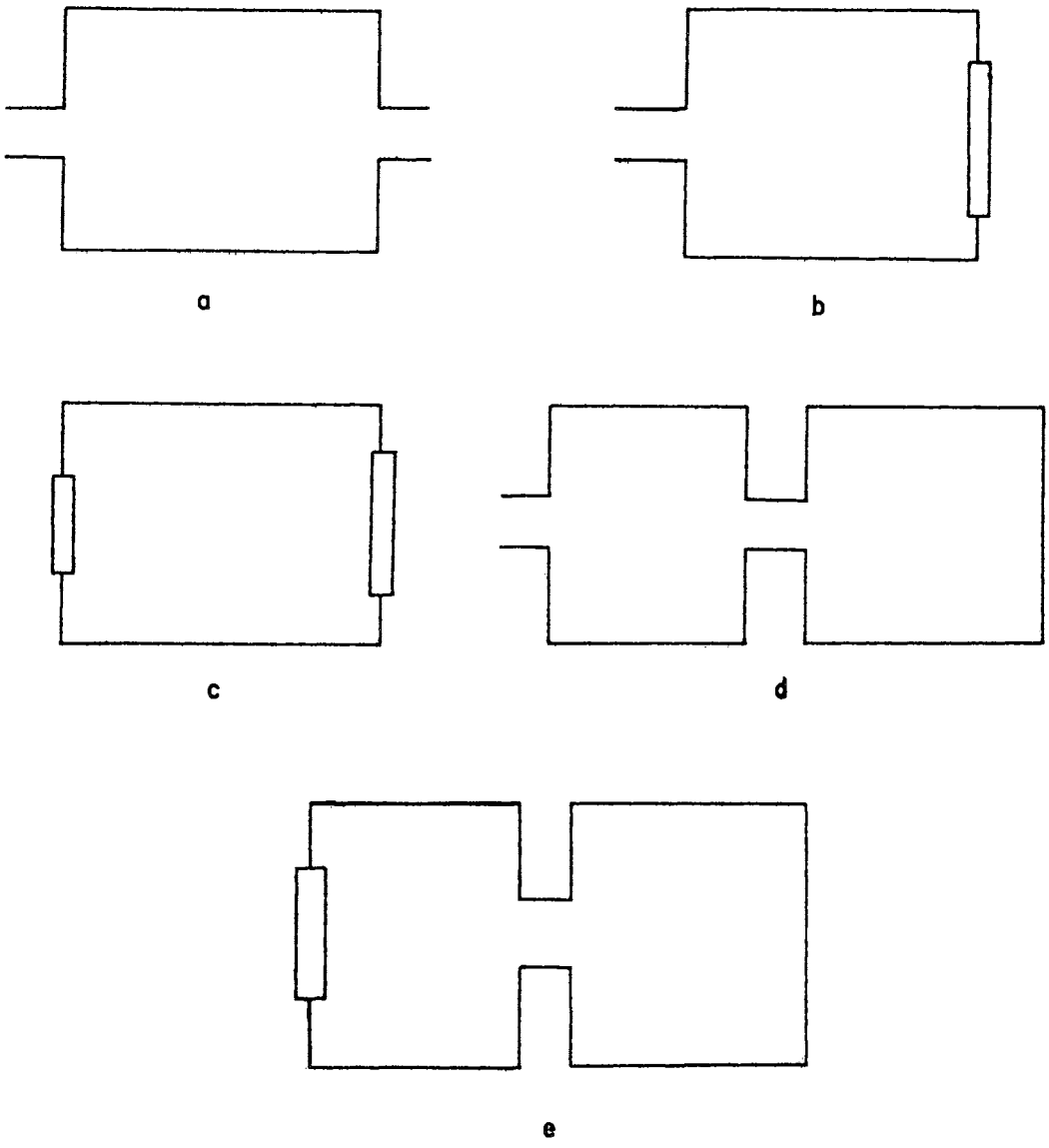

Figure 29. Networks Which Can Be Represented as Two Degree of Freedom Mechanical Systems

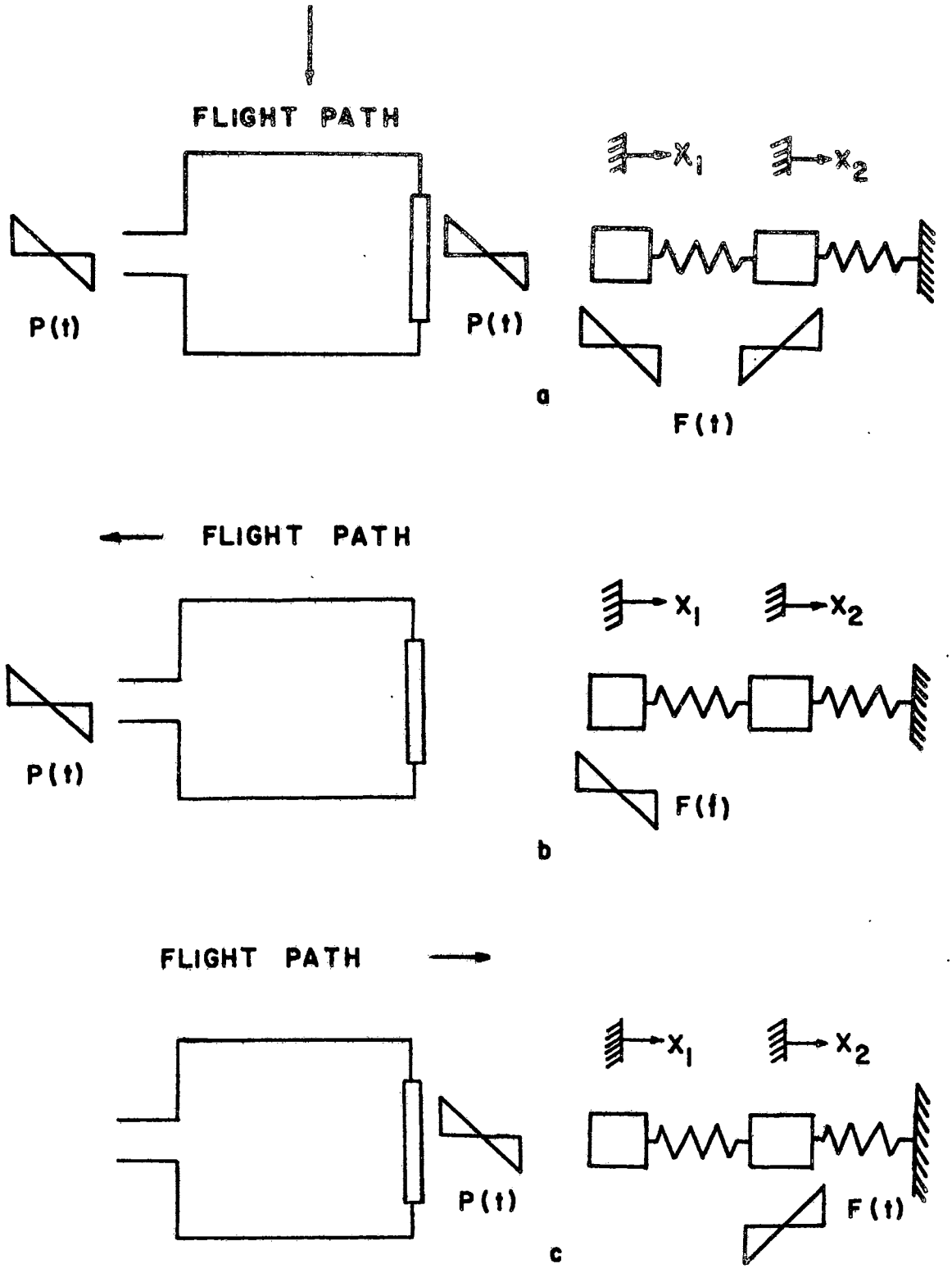

Figure 30. Sonic Boom Loading Conditions

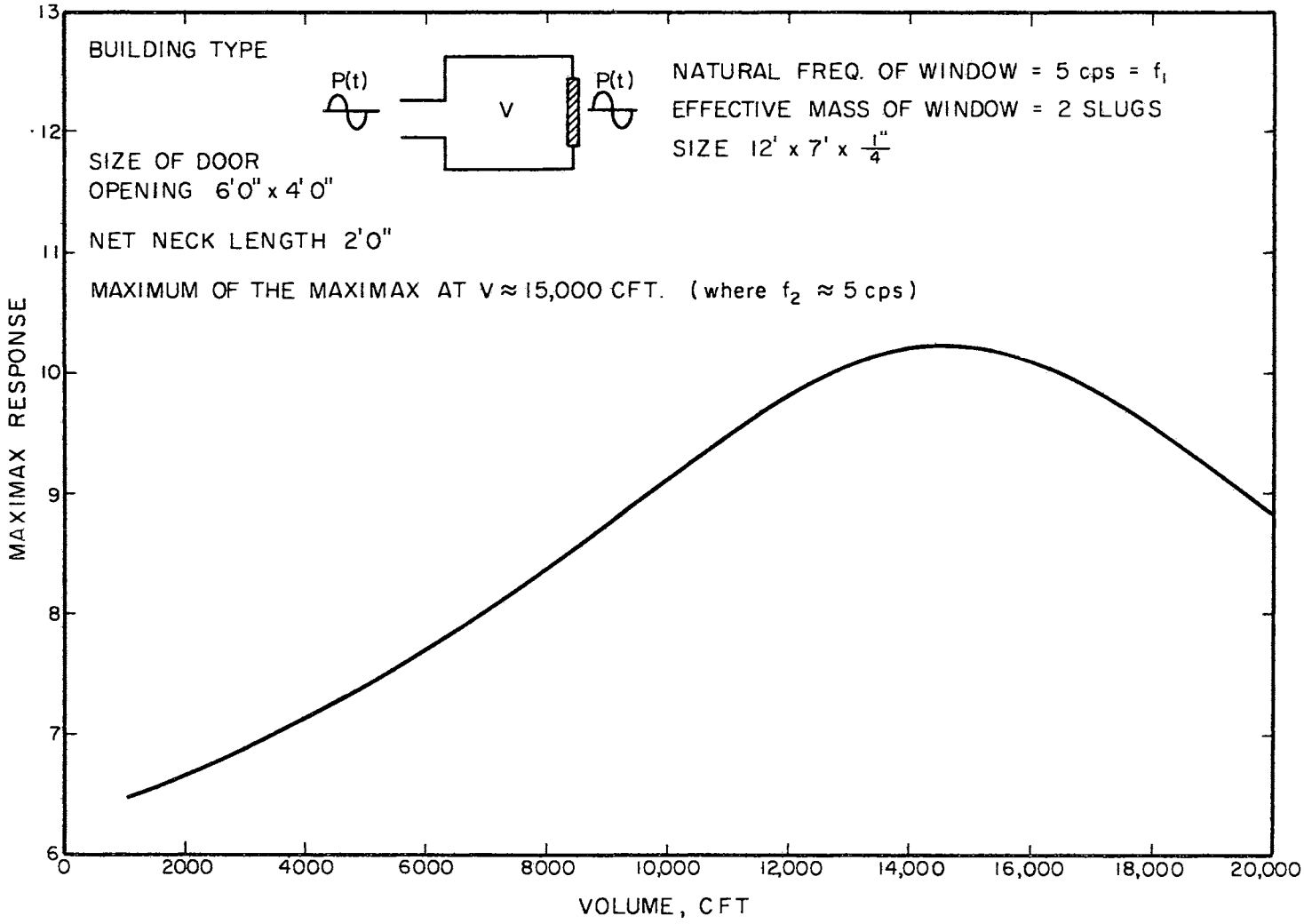

Figure 31. Maximax Response of the Window in a Room with an Opening for Equal and Opposite Sinusoidal Pulse on the Masses

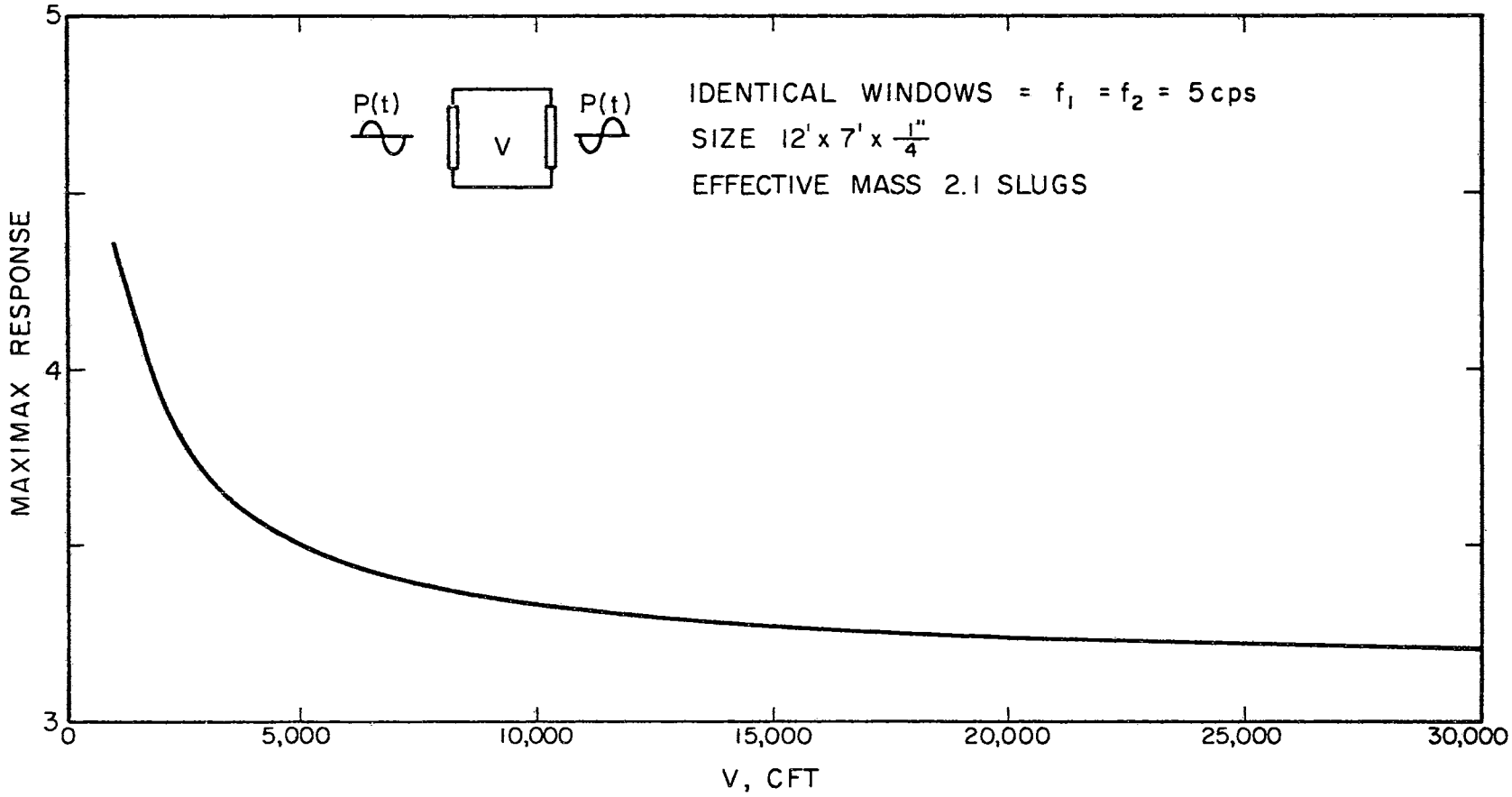

Figure 32. Maximax Response of a Window in a Room with Identical Windows for Similar Sinusoidal Pulse on the Masses

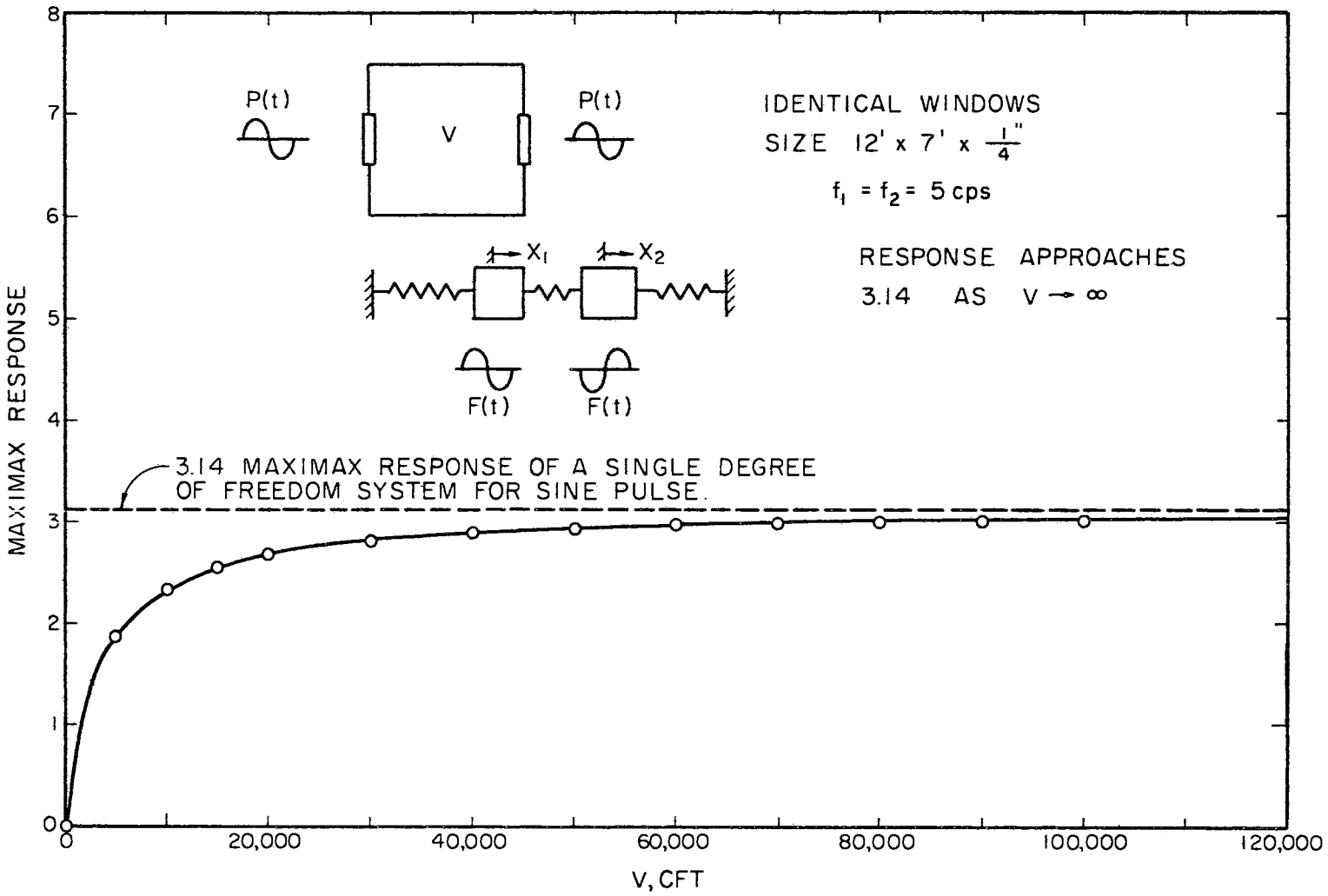

Figure 33. Maximax Response of a Window in a Room with Identical Windows for Equal and Opposite Sinusoidal Pulse on the Masses

maximum response will occur in these. A room with an opening and a window is used to study the critical configuration of an acoustical network later in this chapter.

A Representative Analysis

So far only sinusoidal loads were considered. This was because it was rather easier to analyze for a very general case. For an N-wave excitation an actual system is analyzed using numerical integration. The system and its model are shown in Figure 35.

The equations of motion for the model are,

$$m_1\ddot{x}_1 + C_1\dot{x}_1 + k_1x_1 + k_2(x_1 - x_2) = F_1(t) \qquad (6\text{-}6)$$

$$m_2\ddot{x}_2 + C_2\dot{x}_2 + k_2(x_2 - x_1) = F_2(t) \qquad (6\text{-}7)$$

where m_2 = mass of air in the neck

m_1 = equivalent mass of the window

$k_{2,1}$ = stiffnesses of cavity and panel respectively

C_2 = damping constant at neck

C_1 = damping constant of the panel

L_e = the equivalent length

Damping Constants

The damping constants C_1 and C_2 will be found from the theory developed in Chapter IV. C_2 corresponds to the losses in the neck. The effective radius of the neck is 3.16'. The neck is so wide that the viscous losses are very small and hence can be neglected. The radiation damping ratio is found to be 0.02. C_1 corresponds to the loss mechanisms in the panel. A representative figure of 0.05 is taken

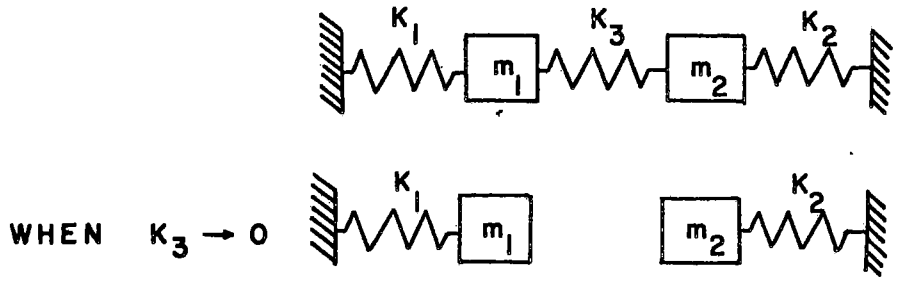

Figure 34. Limiting Case of a Two Degree of Freedom System

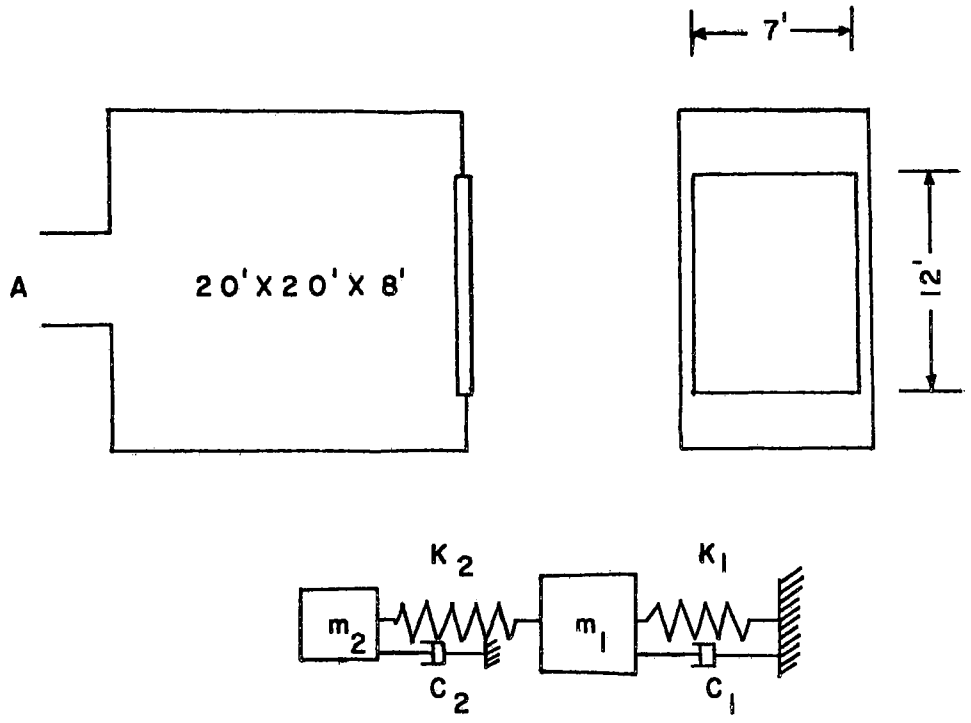

Figure 35. A Representative Mechano-Acoustical System and Its Model

for the damping ratio.

The two equations are solved by numerical integration for equal and opposite N-wave on the masses. The maximum stress in the panel can be calculated from the center deflection. When the period of the N-wave was close to the highest natural period of the system a maximum stress of 841 psi for 1 psf boom is obtained for the undamped case. The corresponding stress for the damped system is 460 psi. An over-pressure of 2.5 is expected for the commercial supersonic transport. This will develop a stress of 2102 psi in the window. Taking a factor of safety of 2.5 (p. 80), the maximum stress in the panel is 5255 psi. This configuration is not critical because the nominal breaking stress of plate glass is 6000 psi.

Comparison of the Experimental Results Obtained from NASA with Theory

Several sonic boom tests were conducted by NASA during the summer of 1966, over two test houses E-1 and E-2 (35) at Edwards Air Force Base. The pressure loadings on the window in the garage of test house E-1, for three different flights, F-104, XB-70, and B-58 are available. The plan of the garage and the corresponding mathematical model are shown in Figure 36.

The door in the garage is assumed to be closed because throughout the discussion in the report by the NASA only single degree of freedom system is mentioned. The equation of motion will be,

$$m\ddot{x} + (C_1 + C_2)\dot{x} + (k_1 + k_2)x = F(t) \qquad (6\text{-}8)$$

C_1 and C_2 are obtained from the representative analysis. The pressure loadings and their straight line approximations are given in Figure 37.

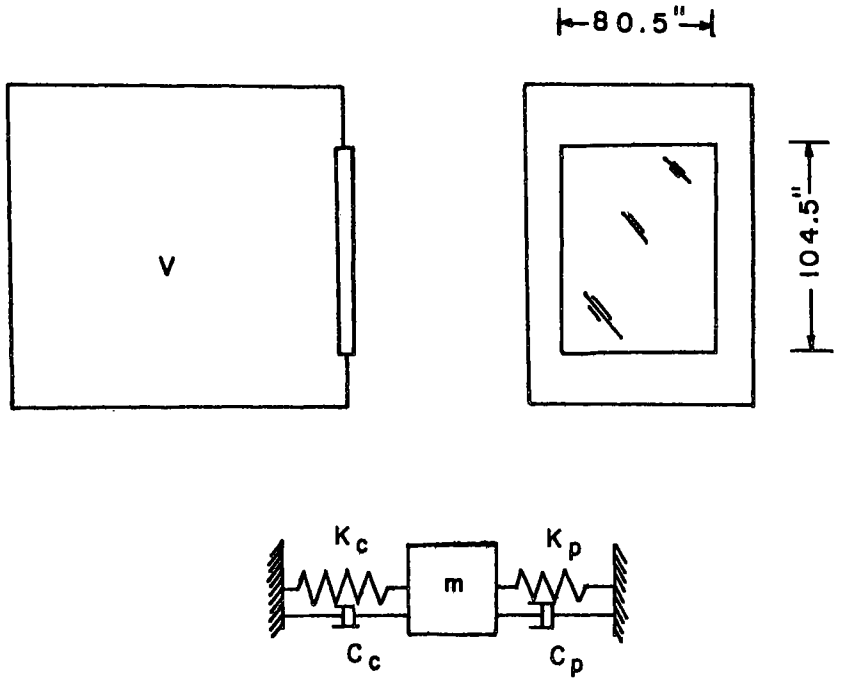

Figure 36. NASA Garage and Its Mechanical Model

The equation of motion is solved numerically and the corresponding ϵ_x calculated for each case. Table IV gives the estimated and measured strains for the three different flights.

TABLE IV

MEASURED AND CALCULATED STRAINS
FOR THE NASA GARAGE WINDOW

Flight	Measured Strain μin/in	Calculated Strain μin/in
XB-70	16.0	24.3
B-58	23.0	26.1
F-104	16.0	28.0

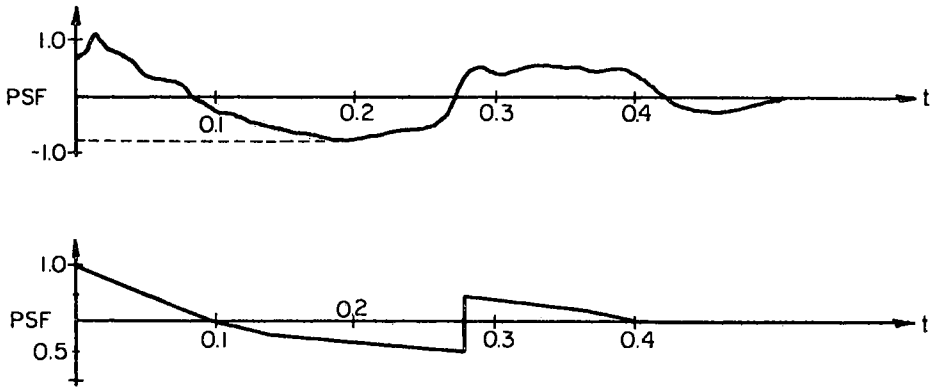

For XB-70

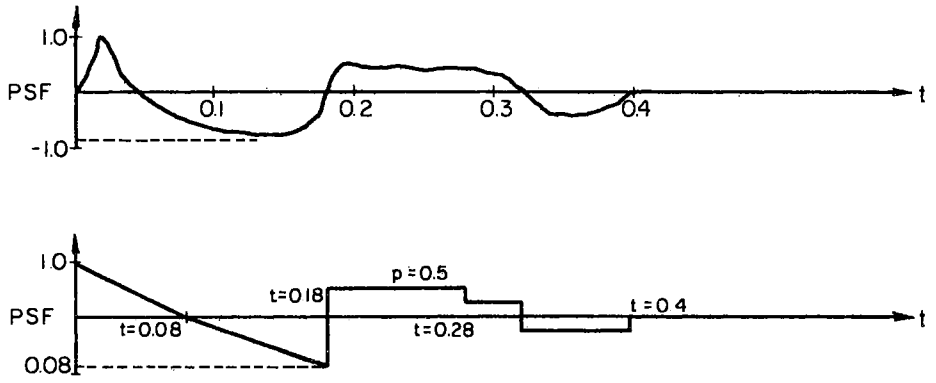

For B-58

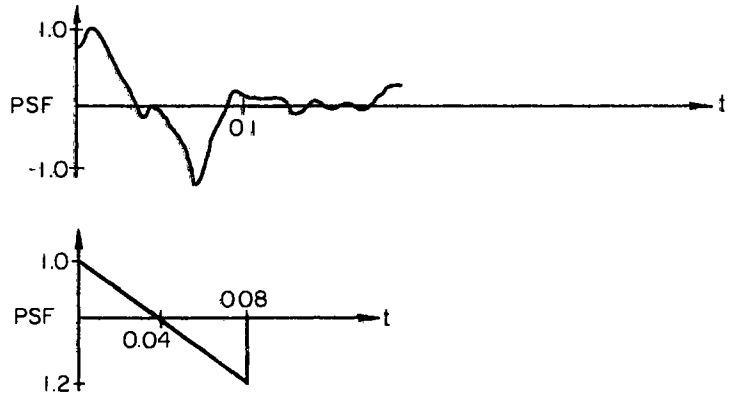

For F-104

Figure 37. Pressure Loadings on the Window in NASA Garage and Their Straight Line Approximations

It is seen that even though the calculated strains are slightly in excess of the measured strains, in no case the strains exceed even a fraction of the damage limit for glass. Since the overpressure was rather small in these three cases (only 1.2 psf), the strain levels are insignificant, probably equivalent to a slight tapping of the window.

The discrepancy between the measured and calculated strains can be explained. Although there will be some error due to the straight line approximation, the main source of error must be in the damping ratio. The window is mounted in a flexible support which moved with the window when it vibrated. This contributes considerably to the damping for which no account is made. Also the flexible ceiling and various tiny leaks in the garage might add up to the total loss. The actual damping ratio could not be measured from the response trace of the strain gage because it is available only for a couple of cycles. In any case theoretical values are not far from the measured ones and can be considered to be an upper limit of response.

The strain gage readings for hundreds of other flights for the windows in test houses E-1 and E-2 are recorded by NASA. But the corresponding pressure loadings are not known. The strains calculated using the pressure readings from the cruciform microphone array (35) are almost twice as great as the measured strains. This is because the windows are located on the sides of the buildings and therefore are not directly under the flight path. A suitable factor has to be used to find the pressure signature near the windows. The maximum strain measured is 37.06 μ in/in which corresponds to 600 psi thus emphasizing that the stress level reached is much lower than the working stress of

glass. If the door was open, slightly higher strains would have been recorded because the system then becomes a two-degree of freedom system whose response is generally greater than 2.16 depending on the system natural frequencies. As explained before the maximax response for a two degree of freedom system will be greater when the two natural frequencies are closer. This means that the mass ratio should be very large. In the following section several two degree of freedom systems where the panel stress exceeds the working stress of glass are found.

Critical Acoustical Systems

In a single degree of freedom system the maximax response to N-wave excitation is limited to 2.16. This corresponds to an equivalent design static load of (2.16x2.5x2.5) 13.50 psf for a 2.5 psf boom. This is much less than the design wind load (30 psf). Therefore failure of the glass panels cannot be expected in such acoustical systems which can be represented as single degree of freedom mechanical systems. In a multi-degree of freedom system the response can take any value depending on the natural frequencies. In Chapter V it was shown that the maximax response of a multi-degree of freedom system is not a function of the number of degrees of freedom but only of the natural frequencies. In order to find a representative system which has the worst response any multi-degree of freedom system with at least two of its natural frequencies nearly the same can be studied. Since a system having two degrees of freedom is the easiest one to analyze for a general case, the critical two degree of freedom practical system will be found.

Again, even in two degree of freedom system it is difficult to

analyze for N-wave in general. The practical acoustical systems which have the greatest response for sinusoidal pulse can be found from the expressions developed in Chapter V. Once a critical system for sinusoidal pulse is obtained, the system for N-wave is obtained by slightly modifying the parameters.

In a two degree of freedom system with a cycle of equal and opposite sinusoidal pulse on the masses the expression for the maximax response is,

$$\frac{\pi p_1^2}{(p_+^2 - p_-^2)} \tag{6-9}$$

This will be large if $\left| p_+^2 - p_-^2 \right|$ is small and p_1^2 large.

Table V gives the critical configurations of several mechano-acoustical systems and the damped and undamped stresses in the window for a sonic boom load of 1 psf. It is found that for a window of size 10'x8'x¾" the damped stress is 1400 psi for a 1 psf boom. This corresponds to a magnification factor of 7.0 and the equivalent design static load on the window will be (7.0 x 2.5 x 2.5) 43.8 psf. So a window designed for a design wind load of 30 psf is likely to fail to a sonic boom of 2.5 psf if the components are properly tuned. Greater magnification ratio than 7.0 can be obtained by reducing the neck area and increasing the window size but these will be only of theoretical interest because all the practical sizes have been considered in Table V.

It is thus found that a properly tuned acoustical system which consists of a door opening and a window is critical for a 2.5 psf boom. The equivalent design static load in this case can be as large as 44 psf. For a room with two windows (identical windows or not) the

TABLE V

MAXIMUM STRESSES IN PANELS
FOR A 1 PSF BOOM

nf	Panel Size	Neck Length Ft.	Neck Area $Ft.^2$	Volume C.Ft.	Maximum Stress psi		T
					Undamped	Damped*	
3.07	15'x15'x1/2"	1.0	10	10000	892	642	0.28
3.74	15'x10'x3/8"	1.0	10	8000	1150	842	0.24
3.52	14'x14'x1/2"	1.0	10	8000	855	608	0 26
4.08	13'x13'x1/2"	1.0	10	6000	789	569	0.22
3.60	12'x12'x3/8"	1.0	10	8000	1170	869	0.24
4.38	12'x10'x3/8"	1.0	10	4000	775	570	0.20
4.87	12'x8 x5/16"	1.0	10	4000	1210	912	0.18
4.31	10'x10'x5/16"	1.0	10	6000	1250	1000	0.20
3.50	10'x10'x1/4"	1.0	10	8000	1540	1200	0.24
5.52	10'x8'x5/16"	1.0	10	4000	1200	980	0.16
4.4	10'x8'x1/4"	1.0	14	9000	1720	1400	0.20
5.4	8'x8'x1/4"	1 0	10	4000	1330	1130	0 16
6.2	8'x7'x1/4"	1.0	18	9000	1380	1155	0.14
7.18	6'x6'x3/16"	1.0	10	2000	1310	1150	0.12
10.4	5'x5'x3/16"	1.0	10	2000	1140	1050	0.10

*2% at the door opening, 4% at the panel.

equivalent design static load never exceeds 30 psf for a 2.5 psf boom. It does not necessarily mean that no failure will occur in such systems because the fatigue effect on glass has not been taken into account.

Failure of Glass

Glass is a brittle material and failure occurs abruptly without yield or permanent deformation. Failure is usually due to the tensile component of the stress exceeding the ultimate strength of the glass. Glass is much stronger in compression than in tension. The variation of breaking stresses in specimens of glass is much greater than for metals. It is because the fractures of glass generally originate in small imperfections or flaws the large majority of which are found on the surface. Any bruise or accidental contact with any hard body will produce on the surface of glass very small cracks which may be invisible even under a microscope. But these micro-cracks act as stress raisers and the stress concentration factor can be as high as 100. In the case of metals because of their ductility the material near these point of concentration yields, thus alleviating the increased stress. But in glass there is no such relief in stress. This is the reason why there is so much variation in the breaking stress of glass. A factor of safety has to be included in estimating the design load. A factor of 2.5 is recommended for all window glasses (26) and this reduces the probability of failure to less than 1%.

Little work has been done on the fatigue of glass. This effect will be more important when a supersonic aircraft flies over an area every half hour, which might happen in a few years. The preliminary work available on the fatigue of glass indicates that it is entirely

different from that of the metals. There is little difference in the stress-time curves of glass under static loading and cyclic loading with complete stress reversal, if the maximum stress and time duration are the same (1). This might indicate that for a short period loading such as the sonic boom, fatigue effect is not much pronounced. But further work is necessary to precisely determine the effect of fatigue.

CHAPTER VII

NON-LINEAR LARGE DEFLECTION THEORY OF PLATES

In the preceding chapters the deflections and the stresses of the panel were found using the linear small deflection theory. This theory is valid strictly for deflections in the range (37),

$$0 < w/h \leqq 0.6$$

where w = deflection at the center and

h = thickness of the panel

For example, a simply supported panel of size 5'x5'x¼" has a central deflection of 0.105" for a 4 psf static load. This corresponds to a w/h ratio of 0.42 and is within the above mentioned limits. Hence linear theory is valid for this case. But now consider a dynamic load, say an N-wave. The maximax response of the model of the panel will be 2.16 and the center deflection for a 4 psf boom will be 0.227". This corresponds to a w/h ratio of 0.90 and hence non-linear theory has to be used. Even the non-linear theory has certain restrictions. For $w/h \gg 1$, membrane theory has to be used. Table VI shows the stress conditions in plates with small, large and very large deflections.

In the first section of this chapter static analysis of plates with large delection is carried out. In the second section an approximate dynamic analysis is made using only the fundamental mode contribution.

TABLE VI

LATERAL STRESSES IN PLATES

	Small Deflection Theory	Large Deflection Theory	Membrane Theory
Stress condition	Bending	Bending and membrane	Membrane
Valid range	$0<w/h\leq 0.6$	$0.6<w/h< 4$	$w/h \gg 1$

Static Analysis of Plates with Large Deflections

The equations of bending of a plate when stretching of the middle plane is taken into account can be found in any advanced text on Theory of Elasticity (37). These are the so-called Von Karman large deflection plate equations and consist of a system of two fourth order non-linear partial differential equations. (7-1 and 7-2)

$$\nabla^4 F = E\left[\left(\frac{\partial^2 w}{\partial x \partial y}\right)^2 - \frac{\partial^2 w}{\partial x^2}\frac{\partial^2 w}{\partial y^2}\right] \tag{7-1}$$

$$\nabla^4 w = \frac{h}{D}\left[\frac{p}{h} + \frac{\partial^2 F}{\partial y^2}\cdot\frac{\partial^2 w}{\partial x^2} + \frac{\partial^2 F}{\partial x^2}\frac{\partial^2 w}{\partial y^2} - 2\frac{\partial^2 F}{\partial x \partial y}\cdot\frac{\partial^2 w}{\partial x \partial y}\right] \tag{7-2}$$

where $\nabla^4 = \left(\frac{\partial^4}{\partial x^4} + \frac{\partial^4}{\partial x^2 \partial y^2} + \frac{\partial^4}{\partial y^4}\right)$

p = lateral loading

h = thickness of the panel

F = stress function such that

N_x, N_y, N_{xy} = normal and tangential loads given by

$$N_x = h\frac{\partial^2 F}{\partial y^2}\ ,\ N_y = h\frac{\partial^2 F}{\partial x^2} \text{ and } N_{xy} = -h\frac{\partial^2 F}{\partial x \partial y}\ .$$

The solution of (7-1) and (7-2) for a general case is unknown. Some approximate solutions are available for a few simplified cases. The two non-linear equations are solved here using the method developed by Kaiser (15). Even though this method can be extended to rectangular plates, for simplicity only square plates are considered. Equations (7-1) and (7-2) can be reduced to four second order linear partial differential equations and a non-linear differential expression by introducing the following non-dimensional quantities.

$$u = x/a$$

$$v = y/a$$

$$p^* = p/E\cdot(a/h)^4$$

$$\Phi = F/h^2E$$

$$\zeta = w/h$$

The reduced equations are,

$$\nabla^2 s = \left(\frac{\partial^2 \zeta}{\partial u \partial v}\right) - \frac{\partial^2 \zeta}{\partial u^2}\cdot\frac{\partial^2 \zeta}{\partial v^2}$$

$$\nabla^2 \Phi = s$$

$$2\frac{\partial^2 \Phi}{\partial u \partial v}\cdot\frac{\partial^2 \zeta}{\partial u \partial v} - \frac{\partial^2 \Phi}{\partial u^2}\frac{\partial^2 \zeta}{\partial v^2} - \frac{\partial^2 \Phi}{\partial v^2}\frac{\partial^2 \zeta}{\partial u^2} = p_G^* \qquad (7\text{-}3)$$

$$\nabla^2 M = 12(1 - \upsilon^2)\,(p^* - p_G^*)$$

$$\nabla^2 \zeta = M$$

The equations are to be solved one after another in the order in which they appear. A deflection surface has to be assumed initially

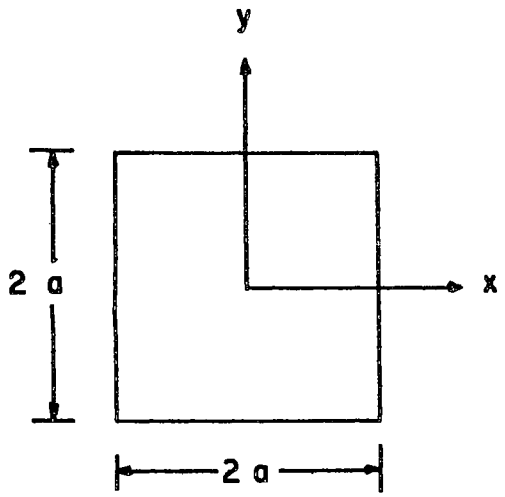

Figure 38. Dimensions of the Plate Used in Deflection Analysis

and this is compared with the result obtained from the last of the equations (7-3). If the difference is considerable a new deflection surface is assumed and the procedure repeated until the results converge to a solution.

Results of the Analysis

Equations (7-3) are solved using the finite differences technique.

Table VII gives the stresses and deflections in panels calculated using linear and non-linear theories. Figures 39 and 40 show the variation of load and stress as a function of deflection for a panel of size 100" x 100" x ¼". It can be concluded from the figures that the load-deflection curve of the panels has a non-linear hard spring characteristic. The stresses and the deflections obtained from the non-linear theory are less than the corresponding values from the

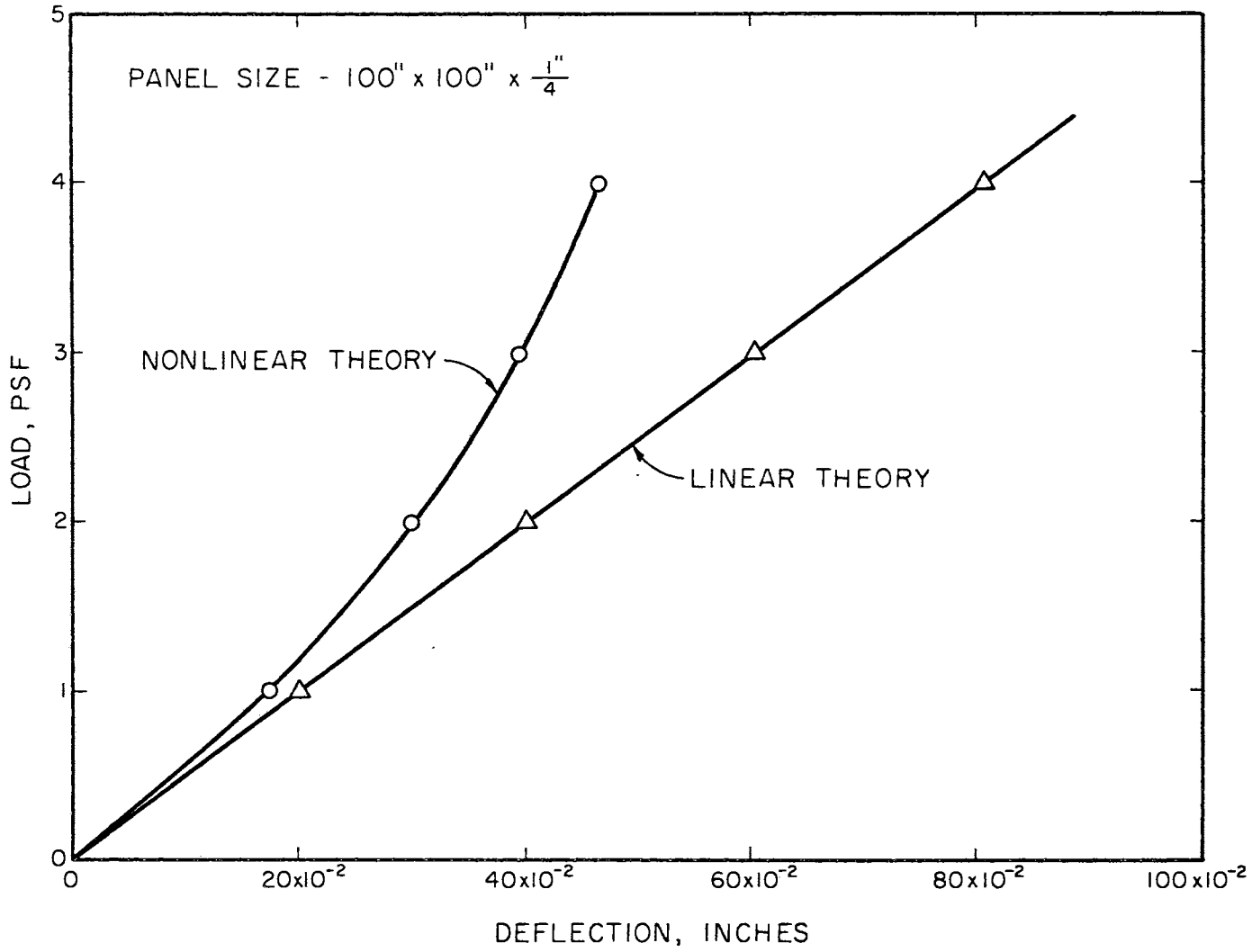

Figure 39. Load-Deflection Curve for a Panel from Large Deflection Theory

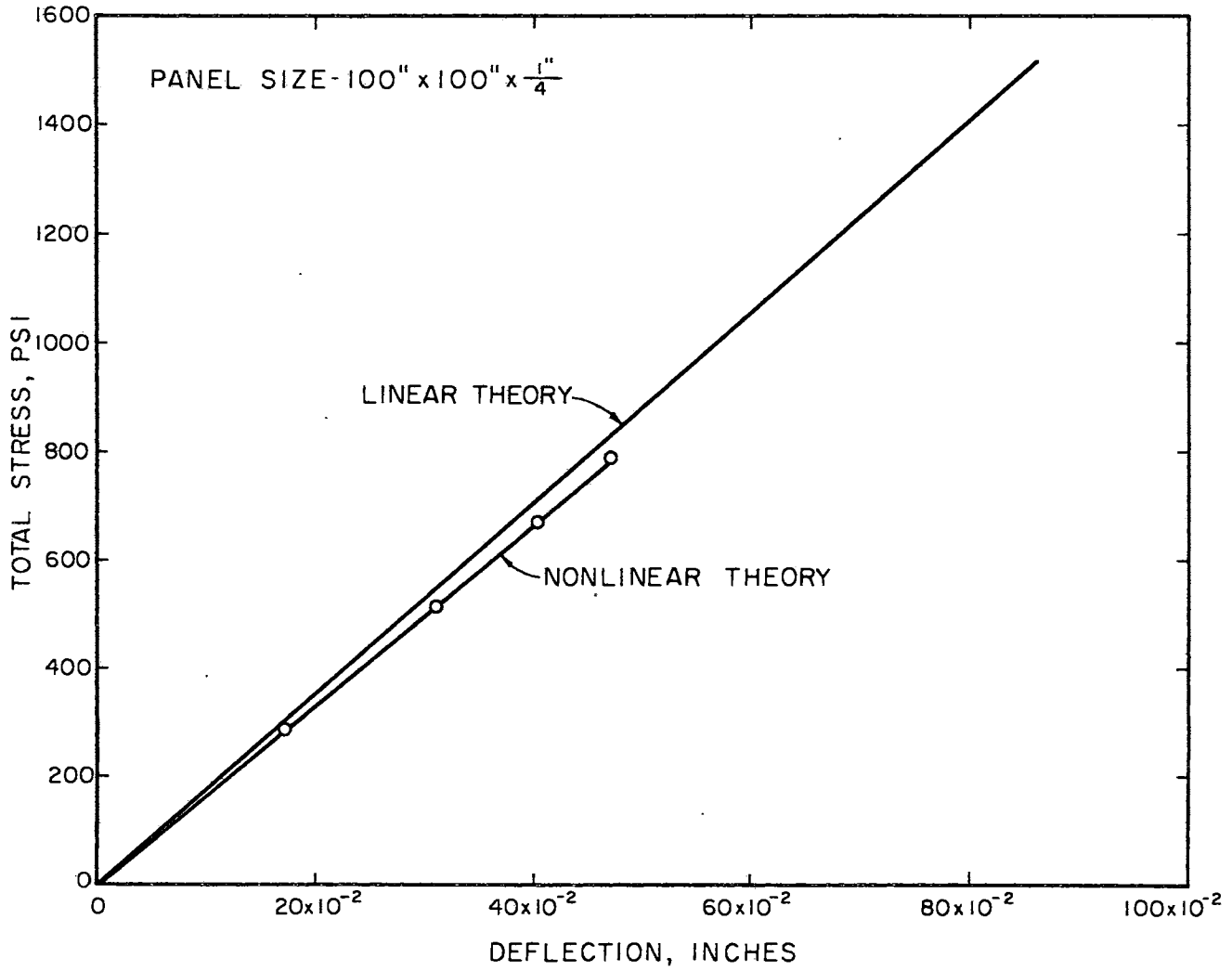

Figure 40. Stress-Deflection Curve for a Panel from Large Deflection Theory

TABLE VII

COMPARISON OF THE STATIC DEFLECTIONS AND STRESSES
OF PLATES USING LINEAR AND NON-LINEAR THEORY

Panel Size	Load	Linear Center Deflection (inches)	Non-Linear Center Deflection (inches)	Linear Max. Stress (psi)	Non-Linear Theory		
					Bending	Membrane (psi)	Total (psi)
20"x20"x¼"	1 psf	.000323	.000307	14.3	12.3	-	12.3
	2 psf	.000646	.000615	28.7	24.6	-	24.6
	3 psf	.000969	.000923	43.0	37.0	-	37.0
	4 psf	.001292	.001230	57.4	49.3	-	49.3
40"x40"x¼"	1 psf	.00516	.00492	57.4	49.3	.7	49.4
	2 psf	.01032	.00984	114.8	98.5	.6	99.1
	3 psf	.01550	.01475	172.2	147.7	1.3	149.6
	4 psf	.02064	.01967	229.6	196.8	2.4	199.2
60"60"x¼"	1 psf	.02615	.02486	129.1	110.6	1.7	112.3
	2 psf	.05230	.04942	258.3	219.3	6.7	226.0
	3 psf	.07845	.07347	387.4	324.6	14.7	339.3
	4 psf	.10460	.09662	516.6	425.2	25.4	450.6
80"x80"x¼"	1 psf	.0826	.07719	229.6	191.9	9.2	201.1
	2 psf	.1652	.14691	459.2	358.5	32.7	391.2
	3 psf	.2479	.2070	688.8	493.2	63.7	556.9
	4 psf	.3304	.25884	918.3	601.0	97.4	698.4
100"x100"x¼"	1 psf	.2018	.1746	358.7	269.9	29.3	299.2
	2 psf	.4036	.29904	707.5	434.6	81.7	516.3
	3 psf	.6054	.3915	1076.2	537.4	133.5	670.9
	4 psf	.8072	.4658	1434.9	608.2	181.7	789.9

linear theory.

Membrane Theory

When the deflection of the panel is much greater than the thickness the bending rigidity approaches zero and all the load is resisted by membrane stresses. The theory developed in the previous section can be used by setting D = 0. Since iteration process is involved again, the simplified membrane bending theory developed by Timoshenko (37) will be used here. From (37), the center deflection of the membrane and the maximum membrane stresses for a simply supported square membrane are given by,

$$w_o = 0{\cdot}802\ a \sqrt[3]{\frac{qa}{Eh}} \tag{7-4}$$

$$\sigma = 0{\cdot}396 \sqrt[3]{\frac{q^2Ea^2}{h^2}} \tag{7-5}$$

where q = lateral pressure loading

2a = side of the membrane

The load-deflection and stress-deflection curves are plotted (Figures 41 and 42) for a membrane of size 180" x 180" x ¼". As in the case of the non-linear theory, the load-deflection curve exhibits a non-linear hard spring characteristic. Further, the membrane stresses are less than the bending stresses calculated using the linear theory.

Transient Response of Panels with Large Deflection

An approximate analysis of the transient response of panels with large deflection is made by deriving an equivalent single degree of

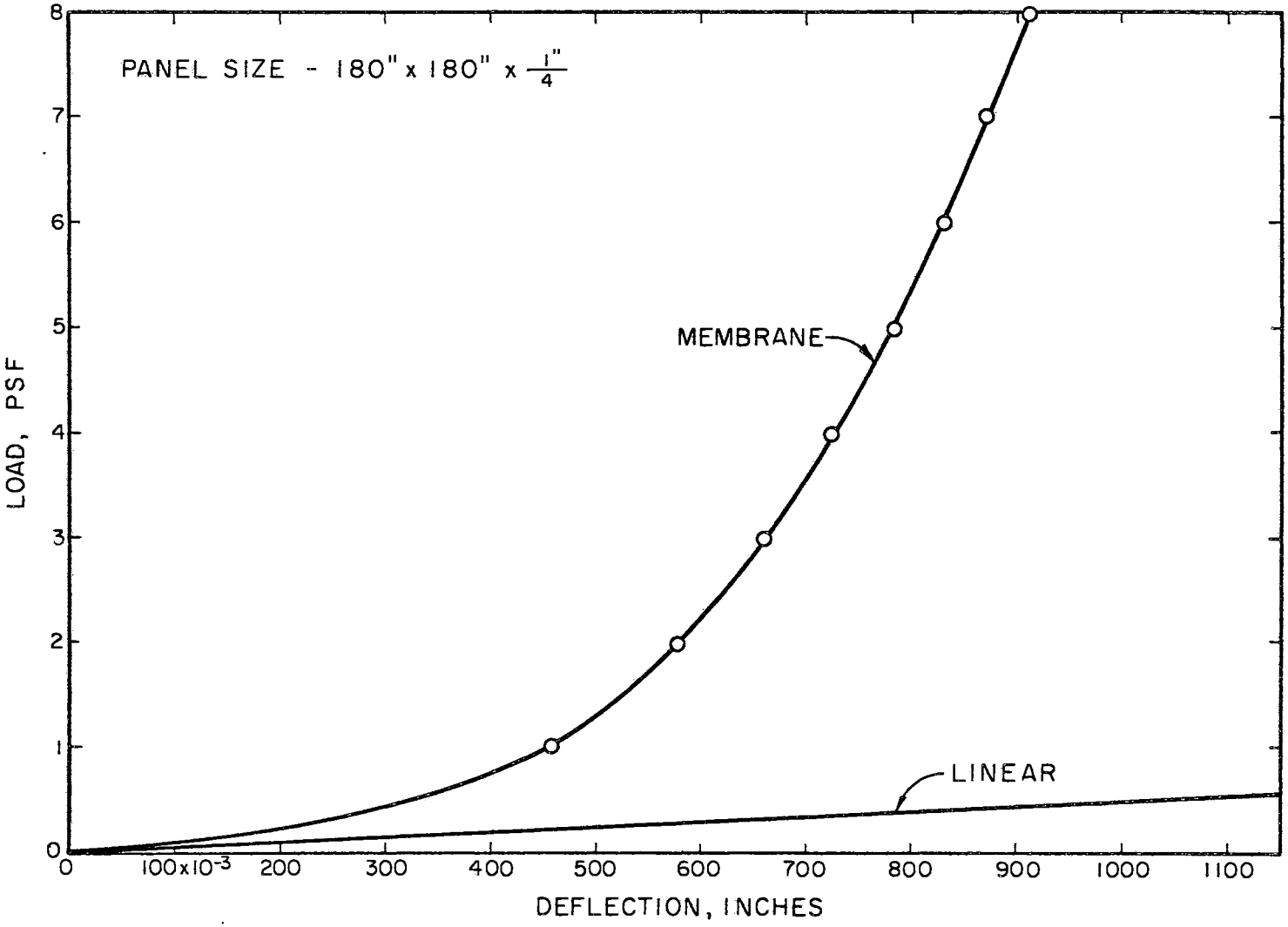

Figure 41. Load-Deflection Curve for a Panel from Membrane Theory

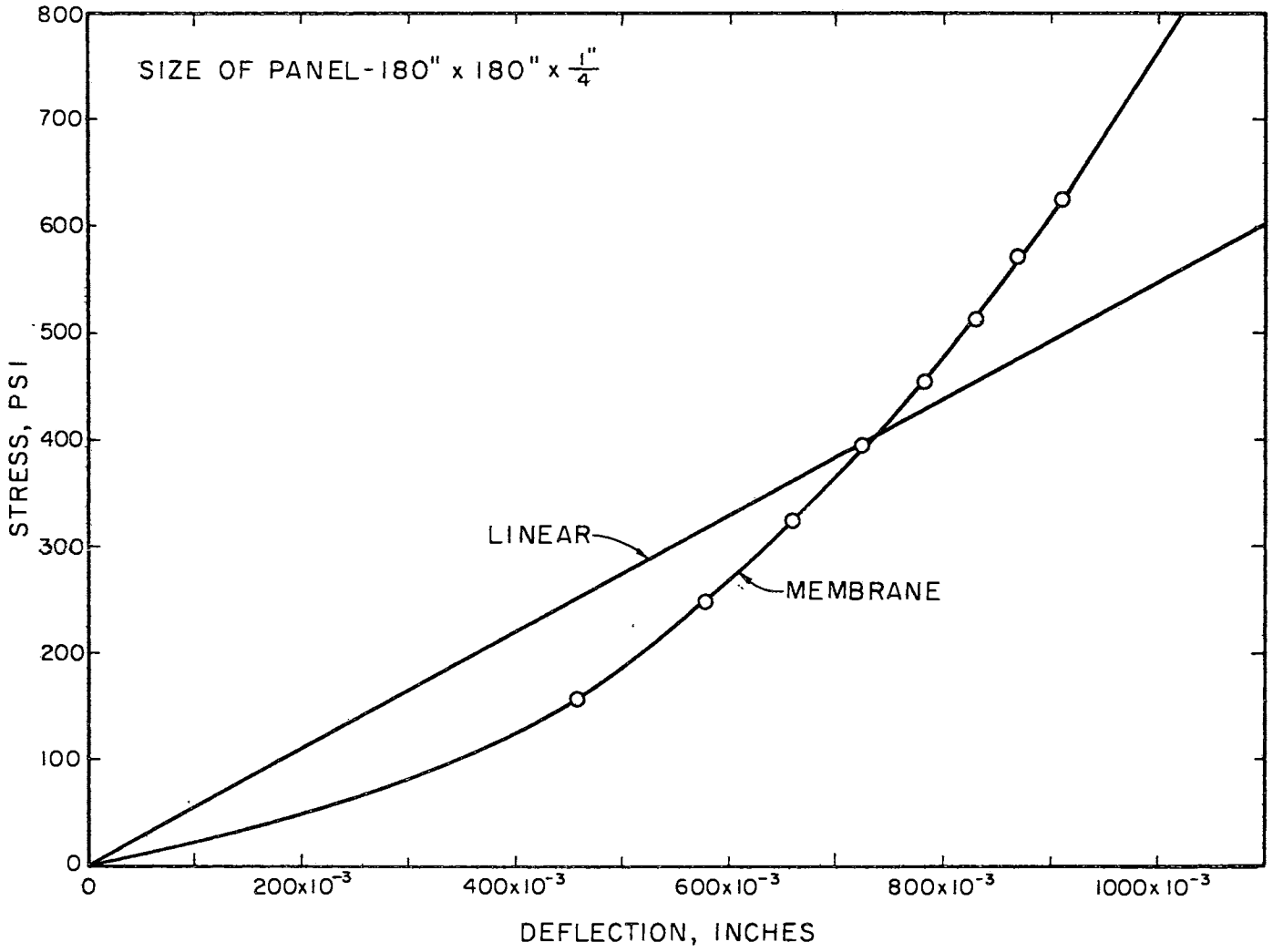

Figure 42. Stress-Deflection Curve for a Panel from Membrane Theory

freedom model. Herrmann and Chu (6) in their analysis on steady state response of panels with large deflections find that the mode shapes can still be taken sinusoidal if the edges are simply supported. The fundamental mode is therefore given by,

$$w_o \text{ Sin } \pi x/a \text{ Sin } \pi y/b \tag{7-6}$$

The equivalent mass can be obtained by equating the kinetic energies as,

$$m_{eq} = m/4 \tag{7-7}$$

The equivalent stiffness is found by equating the potential energies. The load-deflection curve for thin panels and membranes is non-linear and can be represented generally as,

$$F = p \cdot ab = kw + \mu w^3 \tag{7-8}$$

where k = stiffness (in general different from the corresponding value for linear theory)

μ = non-linearity coefficient

The potential energy is given by,

$$\text{P.E.} = \int_o^{w_o} \int_o^b \int_o^a p \text{ Sin } \pi x/a \text{ Sin } \pi y/b \, dx \, dy \, dw \tag{7-9}$$

$$= \frac{4}{\pi^2} \left[k\frac{w_o^2}{2} + \mu\frac{w_o^4}{4} \right] \tag{7-10}$$

Under the assumption that there exists a k_{eq} and a μ_{eq}, the potential energy of a single degree of freedom non-linear (hard spring) system is

$$k_{eq}\frac{w_o^2}{2} + \mu_{eq}\frac{w_o^4}{4} \tag{7-11}$$

This results in,

$$k_{eq} = 4k/\pi^2 \quad \text{and} \tag{7-12}$$

$$\mu_{eq} = 4\mu/\pi^2 \tag{7-13}$$

The equivalent area obtained by preserving the static deflection is,

$$A_{eq} = 4A/\pi^2 \tag{7-14}$$

The equation of motion for the model for an N-wave load is,

$$\ddot{x} + \frac{16}{\pi^2}\left[\frac{kx}{m} + \frac{\mu x^3}{m}\right] = \frac{4}{m\pi^2}ab\left(1 - \frac{2t}{T}\right)p_o \tag{7-15}$$

The stiffness k and the non-linearity coefficient μ can be obtained for different panels from their load deflection curves. (Figures 39 and 41). The corresponding stress is obtained from the stress-deflection curves (Figures 40 and 42). Table VIII gives the results of the dynamic analysis for small panels (large deflection theory) and Table IX gives the results for large panels (membrane theory.)

The stresses predicted by the non-linear theories are much less than the stresses obtained from the linear theory. Hence it can be concluded that the dynamic analysis carried out using the linear theory gives an upper bound for the stresses.

TABLE VIII

STRESSES IN PANELS USING LINEAR AND NON-LINEAR THEORIES FOR N-WAVE LOADING

Load	Panel Size	Deflection (in.)		Total Stress (psi)		w/h
		Linear	Non-Linear	Linear	Non-Linear	
	20"x20"x¼"	134×10^{-5}	128×10^{-5}	59	47	5×10^{-5}
1 psf	60"x60"x¼"	91.5×10^{-3}	85.7×10^{-3}	475	375	0.34
	100"x100"x¼"	0.433	0.350	760	570	1.4

TABLE IX

STRESSES IN PANELS USING LINEAR AND MEMBRANE THEORIES FOR N-WAVE LOADING

Load	Panel Size	Deflection (in.)		Total Stress (psi)		w/h
		Linear	Membrane	Linear	Membrane	
	100"x100"x¼"	0.433	0.356	760	310	1.4
1 psf	120"x120"x¼"	0.917	0.446	1000	345	1.8
	180"x180"x¼"	5.300	0.783	1925	455	3.3

CHAPTER VIII

CONCLUSIONS AND RECOMMENDATIONS

The following conclusions are made from this study.

1. The mathematical model with a mass m/4, stiffness $(\pi^2/4)k$, damping ratio ζ, and area $(4/\pi^2)A$ represents exactly the fundamental mode response of a panel of mass m, stiffness k, damping ratio ζ and area A. The natural frequency (of the fundamental mode) and the static deflection are preserved in the above model.
2. The radiation losses predominate in a wide-mouth resonator and the viscous losses predominate in a narrow-mouth resonator. Hence, in buildings the main damping mechanism at an open door is radiation losses if there are no leaks.
3. The acoustic radiation damping of a simply supported panel is independent of the thickness for a uniform damping pressure and is a function only of the panel aspect ratio. The damping ratio is a minimum for a square panel. The representative acoustic radiation damping ratio of a panel can be taken as 0.001. But, the joint-friction and structural damping of a window are much greater than the acoustic damping.
4. The representative damping ratios for a room with an open door and a window will be 2% at the door and 3% at the window. This forms the lower bound for the damping ratios.

5. The maximax response of mechanical systems is not unbounded when the excitation frequency equals one of the natural frequencies. This maximum is a function of the product of the differences of the squares of the natural frequencies of the system.
6. The severest response in mechanical systems occurs when the loads are acting in a configuration corresponding to the first mode. This means, identical loading conditions on the masses for a symmetrical system. Since the sonic boom loading corresponds to equal and opposite loads on the masses, the response is less severe.
7. The response of a symmetrical two mass three spring system is always less than 2.16 for sonic boom loading. It approaches this value when the stiffness of the center spring is very small. The network which corresponds to the two mass three spring system will be a room with two windows. The maximum response of the windows (if they are identical) for a sonic boom loading is 2.16 which corresponds to an equivalent design static load of 13.5 psf for a 2.5 psf boom. Since windows are generally designed for a 30 psf wind load this configuration is not critical for sonic boom excitation.
8. The maximax response of a two degree of freedom cantilever system can be much greater than 2.16. The exact value is a function of the uncoupled natural frequencies and the mass ratio. This system will correspond to a room with an opening and a window. A magnification factor of 6 10 is obtained for a window in practical acoustical systems. For a panel of size

10'x8'x¼" a stress level of 1400 psi is obtained for a 1 psf boom. This will correspond to an equivalent design static load of 38 psf for a 2.5 psf boom. Hence windows in such systems which are properly tuned yield greater stresses than windows in any other system.

9. The non-linear theory for the panels predicts a hard spring type load-deflection characteristic and the maximax stresses are less than the corresponding values obtained from the linear theory. Hence the stresses obtained from the linear theory represent an upper bound of response.

Recommendations

The following recommendations are made for further study.

1. Since the variation of the breaking stress in several glass panels of the same type is considerable the failure of a plate glass window has to be analyzed statistically.
2. Experimental results for the response to sonic boom can be obtained by simulating sonic booms in buildings of different size and shape.
3. The non-linear transient response of multi-degree of freedom systems needs to be studied.
4. Though the stresses in the window do not exceed the working stress for the glass the possiblity of failure due to fatigue has to be studied. A study of the number of cycles that could exceed the endurance limit for a given sonic boom type can be made.
5. The glass may fail at a much lower stress than the working

stress because of microcracks and other metallurgical flaws which act as stress-raisers. The flow and fracture of glass needs to be studied to understand the failure of glass panels.

6. It has been found in literature on glass that it is possible to increase the working load on glass by pre-compressing it. Pre-compression technique has advanced to such an extent that glass which can resist a stress of 100,000 psi are being made. A study of the suitability of using such glasses in apartment and supermarket windows will be interesting and worthwhile.
7. The transient response of a panel coupled to a cavity has defied exact analysis so far. This can be investigated and the validity of the single degree of freedom assumption for the panel can be verified.
8. The transient response of a panel taking into account additional symmetrical modes is worthwhile because the contribution by the symmetrical modes can be considerable for stress.
9. The stability of the non-linear equations used in the large deflection theory should be studied on a parameter basis so that those equations can be modified suitably to arrive at quick results.
10. In addition to glass breakage, the failure due to sonic booms may be in the form of nail popping and plaster cracking. The exact nature of these is difficult to analyze but approximate predictions can be made.
11. The transient response of a row of panels needs to be studied because most of the supermarket windows are of this type. The one which failed in the sonic boom test in Oklahoma City had

eight windows in a row.

12. It was assumed that the wave length is very long compared to the dimensions of the building. Supermarkets and modern air terminals are almost the same size as the wave length. Exact analysis using the acoustic equation needs to be carried out.

BIBLIOGRAPHY

1. Baker, T. C. and F. W. Preston. "Fatigue of Glass Under Static Loads." Journal of Applied Physics, Vol. 17(3), (1946), pp. 179-188.

2. Bauer, H. F. "The Response of a Non-Linear System to Pulse Excitation." International Journal of Non-Linear Mechanics, Vol. 1 (1966), pp. 267-282.

3. Beranek, L. Acoustics. McGraw Hill Book Company, Inc., 1954.

4. Bies, D. A. and O. B. Wilson. "Acoustic Impedance of a Helmholtz Resonator." The Journal of the Acoustical Society of America, Vol. 25, No. 5 (September, 1953).

5. Cheng, D. H. "Some Dynamic Effects of Sonic Booms on Building Structural Elements." Langley Working Paper, No. 25, NASA.

6. Chu, H. N. and G. Herrmann. "Influence of Large Amplitudes on Free Flexural Vibrations of Rectangular Elastic Plates." Journal of Applied Mechanics, Vol. 78 (1956), pp. 532-540.

7. Crede, C. E. Shock and Vibration Concepts in Engineering Design. Prentice-Hall Inc., 1965.

8. Crocker, M. J. "Theoretical and Experimental Response of Panels to Travelling Sonic Boom and Blast Waves." Wyle Laboratories Report, WR-66-2 (January, 1966).

9. Eisley, J. G. "Non-Linear Vibration of Beams and Rectangular Plates." Zeitschrift für Angewandte Mathematik und Physik, Vol. 15 (1964), p. 167.

10. Ergin, E. I. "Transient Response of a Non-Linear System by a Bi-Linear Approximation Method." Journal of Applied Mechanics, Vol. 78 (December, 1956), p. 635.

11. Fitzgerald, J. V. "Anelasticity of Glass. I: Introduction." Journal of the American Ceramic Society, Vol. 34 (1951).

12. Fung, Y. C. and M. V. Barton. "Shock Response of a Non-Linear System." Journal of Applied Mechanics, Vol. 84(3), (September, 1962), p. 465.

13. Ingard, U. and R. Lyon. "The Impedance of a Resistance Loaded Helmholtz Resonator." The Journal of the Acoustical Society of America, Vol. 25, No. 5 (September, 1953).

14. Johnson, D. R. and D. W. Robinson. "The Subjective Evaluation of Sonic Bangs." Acustica, Vol. 18, No. 5 (1967).

15. Kaiser, R. "Rechnerische und experimentelle ermittlung der durchbeigungen und spannungen von quadratischen platten bei freir auflagerund an den randern, gleichmassig verteilten last und grossen ausbiegungen." Zeitschrift für Angewandte Mathematik und Machanik, Vol. 16 (1936), p. 73.

16. Kornhauser, M. "Prediction and Evaluation of Sensitivity to Transient Acceleration." Journal of Applied Mechanics, Vol. 76 (1954), p. 371.

17. Lamb, H. The Dynamical Theory of Sound. Dover Publications Inc., 1960.

18. Leech, J. W. "Stability of Finite Difference Equation for the Transient Response of a Plate." AIAA Journal, Technical Note, Vol. 3, No. 9 (1965), pp. 1172-1173.

19. Lyon, R. H. "Noise Reduction of Rectangular Enclosures with One Flexible Wall." The Journal of the Acoustical Society of America, Vol. 35, No. 11 (1963).

20. Mangiarotty, R. A. "Acoustic Radiation Damping of Vibrating Structures." The Journal of the Acoustical Society of America, Vol. 35, No. 3 (1965).

21. Marin, G. and G. E. Rindone. "Comparison of Internal Friction of Fiber Glass with Glass Rods." The Glass Industry, Vol. 48, No. 8 (August, 1967).

22. Mayes, W. H. and P. M. Edge, Jr. "Effects of Sonic Boom and Other Shock Waves on Buildings." Materials Research and Standards, Vol. 4, No. 11 (1964).

23. Neubert, V. H. "Lumping of Mass in Calculating Vibration Response." Proceedings of the ASCE, Journal of the Engineering Mechanics Division, EM 1 (1964), p. 47.

24. O'Hara, G. J. and P. F. Cunniff. "Numerical Method for Structural Shock Response." Proceedings of the ASCE, Journal of the Engineering Mechanics Division, EM 2 (1964), p. 51.

25. Orloski, E. "Natural Frequencies of Plate Glass Windows." (Unpublished report, Oklahoma State University, 1967.)

26. Parrott, T. L. "Experimental Studies of Glass Breakage Due to Sonic Booms." Sound, Vol. 1, No. 3 (1962).

27. Pretlove, A. J. "Free Vibrations of a Rectangular Panel Backed by a Closed Rectangular Cavity." The Journal of Sound and Vibration, Vol. 2(3), (1965), pp. 197-209.

28. _____. "Forced Vibrations of a Rectangular Panel Backed by a Closed Rectangular Cavity." The Journal of Sound and Vibration, Vo. 3(3), (1966), pp. 262-276.

29. Rayleigh, J. W. S. The Theory of Sound. Vols. 1 and 2. Dover Publications Inc., 1945.

30. Reddy, N. N. "Response Spectra of Coupled Acoustical Resonators to Transient Excitation." (Ph.D. Thesis, Oklahoma State University, May, 1967.)

31. Samulon, H "Investigations on Acoustic Resonators." The Journal of the Acoustical Society of America, Vol. 19, No. 1 (1947).

32. Simpson, J. D. "The Transient Response of a Helmholtz Resonator with Application to Sonic Boom Studies." (Ph.D. Thesis, Oklahoma State University, May, 1966.)

33. Skipp, B. O. Vibrations in Civil Engineering. London: Butterworths, 1966.

34. Smith, P. W., Jr. and C. Gordon. "Acoustic Losses of a Resonator with Steady Gas Flow." The Journal of the Acoustical Society of America, Vol. 37, No. 2 (1965).

35. Stanford Research Institute. "Interim Report on Sonic Boom Experiments at Edwards Air Force Base." For the National Sonic Boom Evaluation Office (July, 1967).

36. Thomson, W. T. "Shock Spectra of a Non-Linear System." Transactions of the ASME, Journal of Applied Mechanics, Vol. 82(3), (December, 1960), p. 528.

37. Timoshenko, S. and S. Woinowsky-Kreiger. Theory of Plates and Shells. McGraw Hill Book Company Inc., 1959.

38. Ungar, E. E. "Response of Plates to Moving Shocks." Aerospace Engineering (March, 1961).

39. Wang, Chi-Teh. "Non-Linear Large Deflection Boundary Value Problems of Rectangular Plates." NASA Technical Note, No. 1425 (March, 1948).

40 Whitehouse, G. D. "Coupled and Uncoupled Panel Response to Sonic Boom Type Inputs." (Ph.D. Thesis, Oklahoma State University, May, 1967.)

APPENDIX A

NUMERICAL INTEGRATION

Almost all the ordinary differential equations appearing in this thesis were solved using numerical integration. The numerical integration has a great advantage (which compensates for its being a little less accurate) over the conventional Laplace transform method. In the latter method when the excitation frequency equalled one of the natural frequencies of the system erroneous results were obtained for undamped cases. Analytically it was shown that this could not happen and the maximax approached a definite value for a particular system. This value agreed very well with the result obtained from numerical integration.

Numerical integration was performed using the Runge-Kutta and Adams-Moulton methods. The Adams-Moulton method has a better accuracy because it is a predictor corrector method and the solution can be iterated. Since it is not a self-starting method Runge-Kutta method is used to calculate the necessary values for the Adams-Moulton method.

Runge-Kutta Method

There are several orders of Runge-Kutta method depending on the accuracy needed. The error for even the first order method is $0(h^3)$ which is less than the $0(t^2)$ for the Euler method. The method generally used is the fourth-order Runge-Kutta method.

The Runge-Kutta method is derived by assuming a particular form of the solution and equating it to a corresponding Taylor's series solution. The number of terms taken in the Taylor's series depends on the order of the method to be derived. The coefficients of the assumed solution are then obtained by comparing the coefficients of like powers in both solutions.

For an equation of the type,

$$\frac{dy}{dx} = f(x,y) \tag{A-1}$$

with $y(x_o) = x_o$ the fourth-order Runge-Kutta method gives

$$y_{n+1} = y_n + \frac{1}{6}\left[K_1 + 2K_2 + 2K_3 + K_4\right] \tag{A-2}$$

where $K_1 = hf(x_n, y_n)$

$K_2 = hf(x_n + h/2,\ y_n + K_1/2)$

$K_3 = hf(x_n + h/2,\ y_n + K_2/2)$

$K_4 = hf(x_n + h,\ y_n + K_3)$

h = step size

The total truncation error of the Runge-Kutta method is $O(h^5)$.

Adams-Moulton Method

In the Runge-Kutta method every time the derivatives at four different points have to be calculated. The multi-step formulas require only one derivative at each step. This results not only in saving computer time but more accuracy because the solution can be iterated. But the multi-step methods are not self-starting and Runge-Kutta method has to be used to start the process.

The predicted value from the Adams-Moulton method is given by,

$$y^{o}_{n+1} = y_n + \frac{h}{24}\left[55\, f_n - 59_{n-1} + 37\, f_{n-2} - 9\, f_{n-3}\right] \qquad (A\text{-}3)$$

Then f^{o}_{n+1} can be computed because

$$f^{o}_{n+1} = f(x_{n+1}, y^{o}_{n+1}) \qquad (A\text{-}4)$$

The corrected value is given by

$$y^{1}_{n+1} = y_n + \frac{h}{24}\left[9\, f(x_{n+1}, y^{o}_{n+1}) + 19\, f_n - 5\, f_{n-1} + f_{n-2}\right] \qquad (A\text{-}5)$$

The procedure can be repeated and the k^{th} corrected value will be

$$y^{k}_{n+1} = y_n + \frac{h}{24}\left[9\, f(x_{n+1}, y^{k-1}_{n+1}) + 19\, f_n - f_{n-1} + f_{n-2}\right] \qquad (A\text{-}6)$$

The four starting values needed for this method are supplied by the Runge-Kutta method.

If the equations are of higher order or simultaneous, they can be reduced to a number of first order equations and the above procedure can then be used. This method will solve any ordinary differential equation linear or non-linear. A computer program is available with the computer center of Oklahoma State University.

Example

Let the two equations required to be solved be,

$$m_1\ddot{x}_1 + C_1\dot{x}_1 + k_1(x_1 - x_2) = F_1(t) \qquad (A\text{-}7)$$

$$m_2\ddot{x} + C_2\dot{x}_2 + k_2x_2 + k_1(x_2 - x_1) = F_2(t) \qquad (A\text{-}8)$$

These are written in the form

$$\ddot{x}_1 = -\frac{C_1\dot{x}_1}{m_1} - \frac{k_1}{m_1}(x_1 - x_2) + \frac{F_1(t)}{m_1} \qquad (A\text{-}9)$$

$$\ddot{x}_2 = -\frac{C_2\dot{x}_2}{m_2} - \frac{k_2x_2}{m_2} - \frac{k_1}{m_2}(x_2 - x_1) + \frac{F_2(t)}{m_2} \qquad \text{(A-10)}$$

This is a system of two second-order equations and can be reduced to four first-order equations using state variables.

Let

$$y_1 = x_1$$

$$y_2 = \dot{x}_1$$

$$y_3 = x_2 \text{ and}$$

$$y_4 = \dot{x}_2$$

Then the four first-order equations are,

$$\left.\begin{aligned} \dot{y}_1 &= y_2 \\ \dot{y}_2 &= -\frac{C_1y_2}{m_1} - \frac{k_1}{m_1}(y_1 - y_3) + \frac{F_1(t)}{m_1} \\ \dot{y}_3 &= y_4 \\ \dot{y}_4 &= -\frac{C_2y_4}{m_2} - \frac{k_2y_3}{m_2} - \frac{k_1}{m_2}(y_3 - y_1) + \frac{F_2(t)}{m_2} \end{aligned}\right\} \qquad \text{(A-11)}$$

These four first-order equations can then be solved if the four initial conditions are known.

APPENDIX B

FINITE DIFFERENCES TECHNIQUE FOR PANELS FOR STATIC LOADS

The solutions of the plate bending equations for small and large deflection theories using the finite differences technique are discussed here.

Small Deflection Theory

The equation of bending of a plate using small deflection theory is,

$$\nabla^4 w = q/D \tag{B-1}$$

If a square plate is divided into a mesh of size 8 x 8, only ten points have to be considered because of diagonal and rectangular symmetries.

Equation (B-1) can be reduced to two second-order Poisson equations.

$$\nabla^4 F = q/D \tag{B-2}$$

$$\nabla^4 w = F \tag{B-3}$$

The finite difference form of (B-2) (taking the forward differences) is

$$F_{i+1,j} - 4\,F_{i,j} + F_{i-1,j} + F_{i,j+1} + F_{i,j-1} = q/D \tag{B-4}$$

The equations for the ten points in the mesh yield a system of equations the solution of which yields the value of F at all points.

Once F^S are known (B-3) is solved in an identical fashion except for the fact that the right-hand side is replaced by F. Usually it is very easy to solve a linear Poisson equation by the finite differences technique. This is one of the reasons for reducing the non-linear partial differential equations of the plate with large deflection into four Poisson equations and one non-linear differential expression.

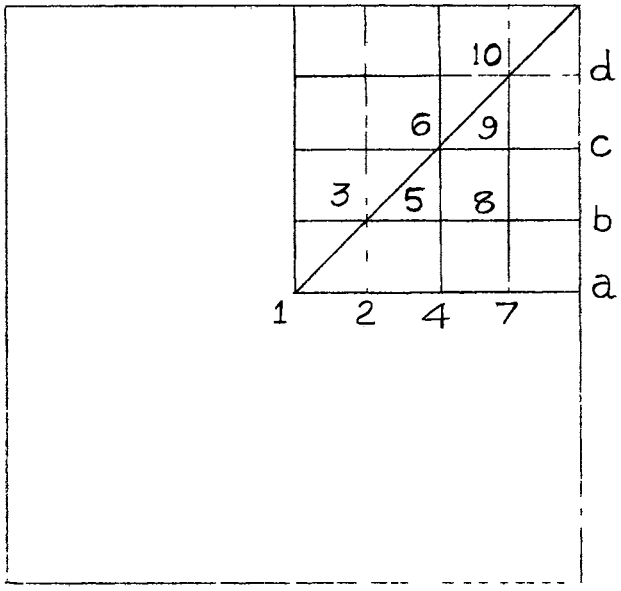

Figure 43. Finite Difference Mesh for a Square Plate

Large Deflection Theory

The finite differences form (taking forward differences) of equations 7-3 is

$$\delta_u^2 s'_{i,j} + \delta_v^2 s'_{i,j} = (\delta_{uv}^2 \zeta_{i,j})^2 - \delta_u^2 \zeta_{i,j}\, \delta_v^2 \zeta_{i,j} \tag{B-5}$$

$$\delta_u^2 \Phi_{i,j} + \delta_v^2 \Phi_{i,j} = s'_{i,j} \tag{B-6}$$

$$2\, \delta_{uv}^2 \Phi_{i,j}\, \delta_v^2 \zeta_{i,j} - \delta_u^2 \Phi_{i,j}\, \delta_v^2 \zeta_{i,j} - \delta_v^2 \Phi_{i,j}\, \delta_u^2 \zeta_{i,j} = p^*_{Gi,j}/n^4 \tag{B-7}$$

$$\delta_u^2 M'_{i,j} + \delta_v^2 M'_{i,j} = \frac{12(1-\upsilon^2)}{n^4} (p^* - p^*_{G\ i,j}) \tag{B-8}$$

$$\delta_u^2 \zeta_{i,j} + \delta_v^2 \zeta_{i,j} = M'_{i,j} \tag{B-9}$$

where $s' = s/n^2$

$M' = M/n^2$

Initially the values of ζ at the ten station points have to be assumed (for $n = 4$). As an initial guess the values given by the linear theory can be taken. Once the deflection surface is known (B-5) becomes a Poisson equation. But it cannot be solved explicitly for s'_1 , s'_2 etc., because of the boundary terms. s'^s are obtained in terms of the values at the boundary. These values of s' are substituted in (B-6) and using the boundary conditions

$$s'_{i\mp1} = 2\Phi_{i,j} \tag{B-10}$$

($i\mp1$ is a boundary point) (B-6) can be reduced to a linear Poisson equation of the type discussed in the linear theory. The solution of this yields Φ. From the non-linear algebraic expression (B-7), p^*_G can be calculated because ζ and Φ are known. (B-8) and (B-9) are then reduced to the linear Poisson equation. The solution of (B-9) yields the deflection surface ζ. This is compared with the assumed ζ and suitable modifications are made and the procedure repeated until desired accuracy is obtained.

Convergence of the Solution

It is found that the method of successive approximation always gave results which were diverging. For example, a simple problem was tried to solve using this method. Let

$$\Phi = \omega^2$$

$$\omega = 1/\Phi \qquad \text{(B-11)}$$

The method of successive approximation yielded results which were oscillating about the exact solution, the oscillations diverging very rapidly.

A method of average successive approximation is therefore used in solving the plate problem. For the second guess

$$\zeta_2 = \frac{\zeta_o + \zeta_1}{2} \qquad \text{(B-12)}$$

was used. The rate of convergence of this method is fairly rapid.

VITA

T. V. Seshadri

Candidate for the Degree of

Doctor of Philosophy

Thesis: TRANSIENT RESPONSE OF MECHANO-ACOUSTICAL NETWORKS

Major Field: Mechanical and Aerospace Engineering

Biographical:

Personal Data: Born in Coimbatore, India, January 30, 1937, the son of T. S. Vaidianathan and Janaki.

Education: Attended schools in Coimbatore, India; graduated from the Municipal High School, Coimbatore, India, in 1951; received the Bachelor of Engineering degree in Civil Engineering from the Madras University, India, in April, 1958; received the Master of Engineering degree in Aeronautics from the Indian Institute of Science, Bangalore, India, in August, 1961; completed the requirements for the Doctor of Philosophy degree in April, 1968.

Professional Experience: Worked as a Civil Engineer for Highways Department, Madras, India, from May, 1958, to July, 1959; as an Aeronautical Engineer in the Hindustan Aircraft Limited, Bangalore, India, from May, 1961, to January, 1965; as Research Assistant at Oklahoma State University from September, 1966, to April, 1968.